Kevin M. Ellis
General Manager
Nuclear Regulatory Affairs, Policy &
Emergency Preparedness

Duke Energy
13225 Hagers Ferry Rd., MG011E
Huntersville, NC 28078

843-951-1329
Kevin.Ellis@duke-energy.com

Serial: RA-23-0242
January 10, 2024

10 CFR 50.55a

U.S. Nuclear Regulatory Commission
ATTN: Document Control Desk
Washington, DC 20555-0001

Catawba Nuclear Station, Unit Nos. 1 and 2
Docket Nos. 50-413, 50-414 / Renewed License Nos. NPF-35 and NPF-52

McGuire Nuclear Station, Unit Nos. 1 and 2
Docket Nos. 50-369, 50-370 / Renewed License Nos. NPF-9 and NPF-17

SUBJECT: Proposed Alternative for the Inspection of Reactor Vessel Closure Head Penetrations in Accordance with 10 CFR 50.55a(z)(2)

Ladies and Gentlemen:

In accordance with 10 CFR 50.55a(z)(2), Duke Energy Carolinas, LLC (Duke Energy) requests U.S. Nuclear Regulatory Commission (NRC) approval of a proposed alternative to certain requirements of the American Society of Mechanical Engineers (ASME) Code, Section XI for Catawba Nuclear Station Units 1 and 2 (CNS) and McGuire Nuclear Station Units 1 and 2 (MNS). Specifically, Duke Energy is requesting relief from the requirements of 10 CFR 50.55a(g)(6)(ii)(D) for the timing of the follow-up examination of the Reactor Vessel Closure Head (RVCH) Penetration Nozzles subsequent to the performance of peening for CNS and MNS. Duke Energy is also requesting an alternative to the depth of compression requirement in the peening performance demonstration criteria of 10 CFR 50.55a(g)(6)(ii)(F)(2)(ii), in which the minimum demonstrated nominal depth of compression is 0.01 inch (0.25 mm).

The proposed alternative is provided in the Enclosure to this submittal. Attachment 1 contains a copy of Calculation No. C-030-2303-00-01, “Axial Crack Growth Evaluation for CRDM Penetration Nozzles in Catawba Unit 2 RVCH.”

Duke Energy requests NRC approval of the proposed alternative within one year of acceptance for review. Should you have any question concerning this letter and its enclosure, please contact Ryan Treadway, Director – Nuclear Fleet Licensing at (980) 373-5873.

No new regulatory commitments have been made in this submittal.

Sincerely,

Kevin Ellis
General Manager, Nuclear Regulatory Affairs, Policy & Emergency Preparedness

Enclosure: Request for Relief related to American Society of Mechanical Engineers (ASME) Code Cases N-729-6 and N-770-5 Augmented Examination Requirements

Attachment:

1. Calculation C-030-2303-00-01, "Axial Crack Growth Evaluation for CRDM Penetration Nozzles in Catawba Unit 2 RVCH."

cc:

L. Dudes, USNRC, Region II Regional Administrator
N. Jordan, USNRC NRR Project Manager for Duke Fleet
J. Klos, USNRC NRR Project Manager for MNS
S. Williams, USNRC NRR Project Manager for CNS
D. Rivard, USNRC Senior Resident Inspector for CNS
C. Safouri, USNRC Senior Resident Inspector for MNS

Enclosure

Duke Energy Carolinas, LLC

Catawba Nuclear Station, Units 1 & 2 and McGuire Nuclear Station, Units 1 & 2

Relief Request RA-23-0242

Relief Requested in Accordance with 10 CFR 50.55a(z)(2)

"Request for Relief related to American Society of Mechanical Engineers (ASME) Code Cases N-729-6 and N-770-5 Augmented Examination Requirements"

1.0 ASME CODE COMPONENT(S) AFFECTED:

Table 1

Unit	Component	Code Class	Examination Category	Item Number
Catawba Nuclear Station, Unit 1 (CNS-1)	Reactor Vessel Closure Head (RVCH) Penetration #1-78 and vent	1	Note 1	B4.60
	RVCH Penetration #79-82	1	Note 2	L
Catawba Nuclear Station, Unit 2 (CNS-2)	RVCH Penetration #1-78 and vent	1	Note 1	B4.60
	RVCH Penetration #79-82	1	Note 2	L
McGuire Nuclear Station, Unit 1 (MNS-1)	RVCH Penetration #1-78 and vent	1	Note 1	B4.60
	RVCH Penetration #79-82	1	Note 2	L
McGuire Nuclear Station, Unit 2 (MNS-2)	RVCH Penetration #1-78 and vent	1	Note 1	B4.60
	RVCH Penetration #79-82	1	Note 2	L

Notes:

1. Examination Items are in accordance with Table 4-3 of MRP-335, Revision 3-A (Reference 8.1) per 10 CFR 50.55a (g)(6)(ii)(D)(*5*).
2. Examination Items are in accordance with Table 4-1 of MRP-335, Revision 3-A per 10 CFR 50.55a (g)(6)(ii)(F)(*2*)(*ii*).

2.0 APPLICABLE CODE EDITION AND ADDENDA:

The reactor vessel closure head (RVCH) at each CNS and MNS unit has 83 total penetrations, i.e., 78 Control Rod Drive Mechanism (CRDM) penetrations, four auxiliary head adapter (AHA) penetrations, and one head vent penetration. The applicable Edition and Addenda of the ASME Code, Section XI (Reference 8.2) for the current ISI interval at each unit is identified in Table 2. 10 CFR 50.55a(g)(6)(ii) specifies augmented examination requirements for pressure boundary components in pressurized water reactors (PWRs) that are fabricated using Alloy 600 base metal and/or Alloy 82/182 weld metals. The RVCH penetration nozzles attached to the closure head by a partial-penetration (e.g., J-groove) weld (Penetrations #1-78 and vent penetration in each head) are examined in accordance with 10 CFR 50.55a(g)(6)(ii)(D), which currently specifies the use of ASME code case N-729-6 (Reference 8.3), with conditions. The Alloy 82/182 butt welds in the AHA penetration nozzles (Penetrations #79-82) are examined in accordance with 10 CFR 50.55a(g)(6)(ii)(F), which currently specifies the use of ASME code case N-770-5 (Reference 8.4), with conditions.

Table 2

Unit	Current ISI Interval	Current Interval ASME Section XI Code Edition/Addenda	Current Interval Start Date	Current Interval End Date[1]	Current License End Date
CNS-1	Fourth	2007 Edition, Through 2008 Addenda	8/19/2015	6/28/2026	12/05/2043
CNS-2	Fourth	2007 Edition, Through 2008 Addenda	8/19/2015	6/28/2026	12/05/2043
MNS-1[2]	Fifth	2007 Edition, Through 2008 Addenda	12/01/2021	11/30/2031	06/12/2041
MNS-2	Fourth	2007 Edition, Through 2008 Addenda	07/15/2014	2/29/2024	03/03/2043

Notes:

1. The Interval End Date is subject to change in accordance with IWA-2430(c)(1) or if a unit transitions from an 18-month fuel cycle to a 24-month fuel cycle.
2. After the first period of the fifth ISI interval, MNS-1 will transition to the 2019 Edition of ASME Section XI.

3.0 APPLICABLE CODE REQUIREMENT:

ASME Code Case N-729-6 contains requirements for the inspection of J-groove welded RVCH penetration nozzles, with or without flaws, as conditioned by Code of Federal Regulations (CFR) 10 CFR 50.55a(g)(6)(ii)(D). ASME Code Case N-770-5 contains requirements applicable to the inspection of the AHA penetrations of RVCHs, with or without flaws, as conditioned by 10 CFR 50.55a(g)(6)(ii)(F). The specific Code requirements for which use of the proposed alternative is being requested are as follows:

N-729-6 Paragraph -2410 specifies that the J-groove welded RVCH penetration nozzles shall be examined on a frequency in accordance with Table 1 of the code case. For Item B4.20, the required extent and frequency of examination is (in part):

> *All nozzles, every 8 calendar years or before RIY=2.25, whichever is less*
>
> *[Note (8)] If flaws are attributed to PWSCC, whether or not acceptable for continued service in accordance with -3130 or -3140, the reinspection interval shall be each refueling outage. For reactor vessel heads with operating temperatures less than 570°F (300°C), the reinspection frequency shall be at least once every 36 months of operating time. Additionally, repaired areas shall be examined during the next refueling outage following the repair.*

Code of Federal Regulations (CFR) 10 CFR 50.55a(g)(6)(ii)(D)(5) requires:

> *Peening. In lieu of inspection requirements of Table 1, Items B4.50 and B4.60, and all other requirements in ASME BPV Code Case N–729–6 pertaining to peening, in order for a RPV upper head with nozzles and associated J-groove welds mitigated by peening to obtain examination relief from the requirements of Table 1 for unmitigated heads, peening must meet the performance criteria, qualification, and examination requirements stated in MRP–335, Revision 3–A, with the exception that a plant-specific alternative request is not required and NRC condition 5.4 of MRP–335, Revision 3–A does not apply.*

MRP-335 Revision 3-A (Reference 8.1, hereafter referred to as MRP-335 R3-A) provides the performance criteria and inspection requirements for peened J-groove welded RVCH penetration nozzles, including incorporation of all conditions in the corresponding NRC Safety Evaluation. Note (11) of Table 4-3 of MRP-335 R3-A addresses the requirement for follow-up examination of peened J-groove welded RVCH penetration nozzles:

> *After peening application, a follow-up examination meeting the inspection requirements of Note 6 shall be performed:*
>
> *(a) in the first and second refueling outages following peening mitigation, for plants with EDY ≥ 8 at the time of peening.*
>
> *(b) in the first and second refueling outages following peening mitigation, for plants with EDY < 8 at the time of peening, if indications of cracking, attributed to PWSCC, have been identified in the RPVHPNs [reactor pressure vessel head penetration nozzles] or associated J-groove welds, whether acceptable or not for continued service under Paragraphs -3130 or -3140 of N-729-1.*
>
> *(c) in the second refueling outage following peening mitigation, for plants with EDY < 8 at the time of peening, if all RPVHPNs in the reactor vessel closure head are free from pre-peening flaws.*

Condition 5.4 introduced the Note (11)(b) to apply for cases with detection of pre-peening flaws. With elimination of condition 5.4 by 10 CFR 50.55a(g)(6)(ii)(D)(5), Note (11)(c) applies regardless of whether pre-peening flaws have been detected. Hence, the current NRC requirement is for a follow-up examination in only the second refueling outage following peening mitigation for plants with EDY < 8 at the time of peening.

For ASME Code Case N-770-5, Code of Federal Regulations (CFR) 10 CFR 50.55a(g)(6)(ii)(F)(*2*)(*ii*) requires:

> *In order to be categorized as peened welds, in lieu of inspection category L requirements and examinations, welds must meet the performance criteria, qualification and examination requirements as stated by MRP–335, Revision 3–A, with the exception that no plant-specific alternative is required.*

The depth of compressive effect for butt welded RVCH penetration nozzles is as required by Section 4.2.8.1.2 of MRP-335 R3-A (in part):

> *The testing shall demonstrate that the nominal depth of the compressive surface residual stress field produced by the peening technique is at least 0.04 in. (1.0 mm).[11] The nominal depth refers to the depth of the compressive residual stress that is reliably obtained in demonstration testing, i.e., for at least 90% of the locations measured.*

Note that Footnote 11 in Section 4.2.8.1.2 of MRP-335 R3-A is not relevant to the cavitation peening method being applied to the reactor vessel closure heads at Catawba and McGuire units.

4.0 REASON FOR REQUEST:

Duke Energy has implemented the peening mitigation process on the CRDM penetrations, vent penetration, and AHA penetrations at CNS-1 in spring 2023 (C1R27), MNS-2 in spring 2023 (M2R28), CNS-2 in fall 2022 (C2R25), and at MNS-1 in fall 2023 (M1R29). Peening was performed on RVCH penetrations #1-78 (CRDM penetrations), the head vent penetration, and RVCH penetrations #79-82 (AHA penetrations). Peening of the RVCH penetration nozzles was performed in accordance with MRP-335 R3-A and meets or exceeds surface stress improvement (SSI) stress requirements for CRDM and head vent penetrations.

Since no flaws attributed to Primary Water Stress Corrosion Cracking (PWSCC) have been identified at CNS-1, MNS-1, and MNS-2, the examination frequency of the CRDM penetrations at these units in accordance with N-729-6 Examination Item B4.20 (i.e., prior to the performance of peening) is every 8 calendar years or before reinspection years (RIY) = 2.25, corresponding to every 4 or 5 fuel cycles at the head temperature applicable to each unit. The four units each operate at reactor cold leg temperature. PWSCC has been previously identified at a CNS-2 CRDM penetration, so the examination frequency at this unit in accordance with N-729-6 Examination Item B4.20 is once every 36 months of operating time (i.e., every 2 fuel cycles prior to the performance of peening). All four RVCHs have accumulated fewer than 8 effective degradation years (EDYs) at the time of peening, so the authorized peening follow-up inspection in accordance with 10 CFR 50.55a(g)(6)(ii)(D)(5) is in the second refueling outage subsequent to peening application (N+2 outage). For the AHA penetrations at each of CNS-1, CNS-2, MNS-1, and MNS-2, N-770-5 Examination Item B-1 requires volumetric examination every second inspection period not to exceed 7 years, and the follow-up examination timing of AHA penetrations must be no sooner than the third (N+3) refueling outage following peening in accordance with MRP-335 R3-A Table 4-1, Item L.

Duke Energy is requesting approval of an alternative to the requirements of 10 CFR 50.55a(g)(6)(ii)(D) to permit performance of the follow-up inspection in the third (N+3) refueling outage rather than the second (N+2) refueling outage subsequent to peening for the MNS-1, MNS-2, CNS-1, and CNS-2 CRDM and head vent penetrations. This alternative would align the CRDM and head vent penetration inspections with the AHA penetration inspections, which are required to be performed no sooner than the N+3 outage after peening. Approval of this request would allow Duke Energy to align the timing of the follow-up inspection of all 83 head penetrations to a single refueling outage, thereby reducing personnel containment entries, risk of working in a Locked High Radiation Area (LHRA), and total personnel collective radiation dose. For these radiological dose and industrial safety concerns and based on the assessments and supplemental evaluations described in Section 5.0 of this relief request, performance of the follow-up inspection for the 78 CRDM penetrations and vent penetration on the schedule required by MRP-335 R3-A is considered a hardship without a compensating increase in the level of quality and safety in accordance with 10 CFR 50.55a(z)(2).

Because of the limited access to the inside of RVCH penetration nozzles, MRP-335 R3-A specifies a minimum peening nominal compressive residual stress depth of 0.01 inch (0.25 millimeter) for RVCH penetration nozzles. However, as access to the interior of piping butt welds being peened is not limited, MRP-335 R3-A specifies a minimum peening nominal compressive residual stress depth of 0.04 inch (1.0 millimeter) for Alloy 82/182 piping butt welds. In combination with the performance criteria for surface stress (applied and residual) subsequent to peening, the compressive depth criteria ensure peening is effective to prevent future PWSCC initiation.

Duke Energy is also requesting approval of use of an alternative performance criterion for the qualification of the peening compressive residual stress depth for the Catawba and McGuire units. Duke Energy requests to use a minimum nominal compressive residual stress depth of 0.01 inch (0.25 millimeter) for the AHA penetrations at each of MNS-1, MNS-2, CNS-1, and CNS-2 instead of the depth of 0.04 inch (1.0 millimeter) specified in Section 4.2.8.1.2 of MRP-335 R3-A for Alloy 82/182 piping butt welds. For the AHA penetrations, the nozzle geometry and access limitations make obtaining a compressive residual stress depth of 0.04 inch (1.0 millimeter) impractical for some of the welds using the peening technology being applied at the Catawba and McGuire units. Providing that all other performance criteria, qualification, and examination requirements stated in MRP-335 R3-A are met per 10 CFR 50.55a(g)(6)(ii)(F)(*2*)(*ii*), the proposed alternative would permit the subsequent volumetric examinations, after the follow-up examination, of AHA penetrations on a frequency of each ISI interval (same as for peened CRDM and vent penetrations) instead of the frequency of every second inspection period not to exceed 7 years per N-770-5 Item B-1. Hence, the proposed alternative compressive residual stress depth criterion would facilitate long-term alignment of the head examinations at each unit, thereby reducing personnel containment entries, risk of working in a Locked High Radiation Area (LHRA) and total personnel collective radiation dose. For these radiological dose and industrial safety concerns and based on the assessments described in Section 5.0 of this relief request, the depth of compression required by the performance criteria in Section 4.2.8.1.2 of MRP-335 R3-A is considered a hardship without a compensating increase in the level of quality and safety in accordance with 10 CFR 50.55a(z)(2).

5.0 PROPOSED ALTERNATIVE AND BASIS FOR USE:

Proposed Alternative is as Follows:

Pursuant to 10 CFR 50.55a(z)(2), Duke Energy is requesting relief from the requirements of 10 CFR 50.55a(g)(6)(ii)(D) and 10 CFR 50.55a(g)(6)(ii)(F) for the timing of the follow-up examination of the RVCH penetration nozzles subsequent to the performance of peening (CRDM penetrations #1-78 and head vent) and for the minimum nominal compressive residual stress depth requirement (AHA penetrations #79-82). Specifically, Duke Energy is requesting a one-time alternative to the examination frequency requirements of 10 CFR 50.55a(g)(6)(ii)(D)(5), in which a single post-peening follow-up examination of the CNS-1, CNS-2, MNS-1, and MNS-2 RVCH penetrations identified in Table 1 is performed in the third (N+3) refueling outage after peening. Duke Energy is also requesting an alternative to the depth of compression requirement in the peening performance demonstration criteria of 10 CFR 50.55a(g)(6)(ii)(F)(*2*)(*ii*), in which the minimum demonstrated nominal depth of compression is 0.01 inch (0.25 mm).

In accordance with 10 CFR 50.55a(g)(6)(ii)(D)(*5*) and (F)(*2*)(*ii*), Duke Energy shall confirm that the performance criteria, qualification, and examination requirements stated in MRP-335 R3-A are satisfied, with the exception that a plant-specific alternative request is not required and NRC condition 5.4 of MRP-335 R3-A does not apply, prior to obtaining examination relief from the requirements of 10 CFR 50.55a(g)(6)(ii)(D) and (F) for unmitigated RVCH penetrations. The two requested alternatives represent limited proposed modifications to the MRP-335 R3-A requirements specific to the CNS and MNS heads.

A relevant indication was identified via volumetric ultrasonic leak path (UTLP) and confirmed via eddy current testing (ET) of the J-groove weld surface in RVCH Penetration #74 at CNS-2 in the spring 2021 (C2R24) refueling outage. This apparent leak was not detected by subsequent bare metal visual examination, and the leak was not accompanied by any visually discernible low-alloy steel corrosion or circumferential cracking within the nozzle tube. To address the detected indication of PWSCC, an embedded flaw repair (EFR) was performed of RVCH Penetration #74 at CNS-2 during the spring 2021 (C2R24) refueling outage. The outer surfaces of this penetration (outside diameter of the nozzle and J-groove weld and butter surface) were overlaid with PWSCC-resistant Alloy 52/52M weld metal. No peening of the outer surfaces of RVCH Penetration #74 at CNS-2 was necessary because, as stated in Reference 8.5, the Alloy 52/52M seal weld extends down to the top of the thread relief region on the nozzle tube. The examination requirements applicable to this single repaired penetration are specified within Relief Request RA-21-0144 (Reference 8.6).

In Reference 8.7, NRC approved the use of the proposed alternative RA-21-0144 for the remainder of the current fourth ISI interval at CNS-2.

The nondestructive examination requirements for Penetration #74 at CNS-2 specified by RA-21-0144 include periodic UT examination of the nozzle tube consistent with 10 CFR 50.55a(g)(6)(ii)(D) and periodic surface examination of the EFR. The UT examination is specified for the refueling outage following implementation of the repair, with a subsequent UT examination frequency "consistent with 10 CFR 50.55a(g)(6)(ii)(D), which requires implementation of Code Case N-729-6 with conditions, or NRC-approved alternatives." The UT examination specified for the refueling outage following implementation of the repair was completed during the fall 2022 (C2R25) refueling outage at CNS-2 when the inner surfaces of this penetration were peened along with the other RVCH penetrations at CNS-2. The exposed PWSCC-susceptible surfaces (i.e., the nozzle inside diameter surfaces) of the repaired RVCH Penetration #74 at CNS-2 required to be peened have been peened. If the requirements of Section 4.3 of MRP-335 R3-A are satisfied, a RVCH penetration with flaws that has been corrected and subsequently peened using a process meeting the performance criteria of Section 4.3.8 of MRP-335 R3-A may be identified as Item B4.60 in Table 4-3 of MRP-335 R3-A (see Section 4.3.7 and Note (12) of Table 4-3 of MRP-335 R3-A). Hence, under the proposed alternative N+3 timing for the UT examination following peening, the next UT examination of RVCH Penetration #74 at CNS-2 would be during the third refueling outage following peening when the next UT examination is performed of the other penetrations. The subsequent UT examinations of RVCH Penetration #74 at CNS-2 would be performed on the frequency in accordance with the requirements for peened RVCH penetrations per 10 CFR 50.55a(g)(6)(ii)(D)(*5*). As stated above, Duke Energy shall confirm that the applicable performance criteria, qualification, and examination requirements are met prior to obtaining examination relief from the requirements of 10 CFR 50.55a(g)(6)(ii)(D) and (F) for unmitigated RVCH penetrations. Periodic surface examinations of the EFR will be continued during the fourth ISI interval in accordance with RA-21-0144 (Reference 8.6) and the associated NRC Safety Evaluation (Reference 8.7).

The Basis for the Proposed Alternative is as Follows:

Each of the Affected Components is an Alloy 600 penetration nozzle welded to the low-alloy steel RVCH using Alloy 82 and/or 182 weld metal. The penetrations are located in the cold leg temperature (T_{cold}) region of the reactor coolant system (RCS). Operating at T_{cold} has a large benefit for reducing PWSCC susceptibility and extending PWSCC crack growth time compared to a penetration in a RVCH operating near hot leg temperatures. A limited number of PWSCC indications affecting Alloy 600 RVCH penetrations at T_{cold} temperatures have been reported in U.S. PWRs, and in none of these cases has visually discernible corrosion of the low-alloy steel head been reported.

Hardship

The components listed in this request are located inside containment and in areas involving occupational radiation exposure. Volumetric examination of RVCH penetration nozzles requires personnel exposure during examination equipment set-up, during examination, and during demobilization of the equipment. Volumetric examination of the 78 CRDM penetrations and vent penetration in a separate outage than the four AHA penetrations at each unit would require an unnecessary increase in worker radiation exposure since similar equipment set-up, demobilization, and tool change-out activities are required for each of these activities. The increase in exposure represents an activity adverse to As-Low-As Reasonably Achievable (ALARA) program practices. To align the examinations, an alternative to the required N+2 follow-up inspections for the CRDM and vent penetrations is requested to align with the required N+3 follow-up inspection for the AHA penetrations, and an alternative to the depth of compressive residual stress performance criterion for the AHA penetrations is also requested recognizing the hardship of the impracticality of obtaining the nominal depth of 0.04 inch (1.0 mm) specified in MRP-335 R3-A for Alloy 82/182 piping butt welds.

Based on historical data at CNS-2, the additional occupational dose if volumetric examination of the AHA penetrations were performed in a separate outage from the other RVCH penetration nozzles is estimated to be approximately 250 to 300 mRem more than examining all RVCH penetration nozzles in the same outage. This estimate includes exposure due to set-up and demobilize equipment. Additional exposure is expected due to examination activities such as tool change-out and expected probe failure changes. An even higher dose would be expected if difficulties during examination are experienced or if execution abnormalities occur due to a potential tool breakdown requiring LHRA entry and subsequent additional dose accrual.

In summary, performance of the follow-up examinations for the J-groove and butt-welded nozzles in two separate outages results in a hardship that is not compensated for by a corresponding increase in safety or quality. In addition, performing inspections in two separate outages could introduce potential hazards to personnel safety for the following reasons:

1. Requires additional radiation exposure due to entry inside containment. The increase in dose is estimated to be approximately 250 to 300 mRem based on historical data but can be higher if tool breakdowns or issues occur requiring additional personnel entry, which is inconsistent with industry ALARA practices.
2. Combining two inspections to one inspection reduces risk of industrial accidents. Fewer number of containment and LHRA entries and potential entries to LHRA decreases the potential for industrial safety risks.
3. Potential for increases in contamination exposure due to entries inside containment and entry to LHRA.

Duke Energy has concluded that performance of a follow-up inspection in the N+2 refueling outage for the CRDM penetrations and vent penetration and in the N+3 outage for the AHA penetrations constitutes a hardship without a compensating increase in the level of quality and safety. The proposed alternative to perform the follow-up inspection for all penetrations (Section 1.0) in the N+3 refueling outage is supported by the assessments and supplemental evaluations presented in the following sections. Moreover, the compressive residual stress depth criterion for Alloy 82/182 piping butt welds of MRP-335 R3-A in the case of the AHA penetrations represents a second hardship without a compensating increase in the level of quality and safety. The proposed alternative performance criterion is also supported by the assessments and supplemental evaluations presented below.

Assessment of Operating Experience for J-groove Welds Operating at T_{cold}

Through consideration of a matrix of deterministic PWSCC crack growth calculations, MRP-335 R3-A shows how the timing of volumetric examinations subsequent to peening are effective to prevent pressure boundary leakage. The matrix of cases considers the growth of hypothetical, shallow PWSCC flaws located in the nozzle Alloy 600 base metal that exist at the time of peening. The hypothetical flaws are too shallow to be reliably detected in the pre-peening baseline inspection. The evaluation per TN-4069-00-01 (Reference 8.8), which is based on the crack growth results available in Section 5.2.3.2 of MRP-335 R3-A, investigates how effective the N+1 or N+3 follow-up inspection timing would be compared to the N+2 follow-up inspection timing in the case of heads operating at reactor cold-leg temperature (T_{cold}) with a nominal 18-month fuel cycle to prevent through-wall cracking and pressure boundary leakage. (Each of the CNS and MNS units operates on a nominal 18-month fuel cycle.) The identical low fraction of deterministic cases in the matrix for RVCH penetration nozzles operating at T_{cold} shows cracking of a size causing leakage assuming the N+3 timing as often as assuming the N+2 timing, demonstrating how the N+3 timing would ensure a similarly low likelihood of leakage. The crack growth results also show that N+1 follow-up examination timing is not as effective as N+2 or N+3 timing as growth of shallow PWSCC flaws over a period of 18 months for T_{cold} heads may not be sufficient for the flaw to become deep enough to be reliably detectable using ultrasonic testing (UT).

The experience for unmitigated heads in the U.S. operating at T_{cold}, including that for the CNS and MNS heads prior to peening, shows that in practice and without taking credit for the peening surface stress improvement, cracking causing leakage of the Alloy 600 base metal is unlikely to occur prior to an alternative N+3 follow-up inspection. A 2016 PVP conference paper (Reference 8.9) evaluated in detail the PWSCC indications detected in 25 RVCH penetration nozzles in T_{cold} heads by that time, all in the area of the toe of the J-groove weld on the nozzle outside diameter (OD). Through an extension of the assessment of plant experience in the PVP paper, the evaluation in TN-4069-00-02 (Reference 8.10) demonstrates how substantial margin against growth upward to the nozzle annulus and against consequential leakage would still be expected with a 4.5-year inspection (i.e., N+3 for units with nominal 18-month fuel cycles). It is noted that limited Alloy 600 nozzle base metal cracking has been observed since these analyses were performed, and the analyses remain applicable.

As mentioned above, a relevant indication was identified via volumetric ultrasonic leak path (UTLP) and confirmed via eddy current testing (ET) of the J-groove weld surface in RVCH Penetration #74 at CNS-2 in the spring 2021 (C2R24) refueling outage. This apparent leak was not detected by subsequent bare metal visual examination, and the leak was not accompanied by any visually discernible low-alloy steel corrosion or circumferential cracking within the nozzle tube. No indications of PWSCC were detected in the volumetric examination of the nozzle base metal, which is the focus of the required periodic volumetric examinations.

Application of Alternative Follow-Up Interval to CNS-1, MNS-1, and MNS-2

As stated in Section 4.0, no flaws attributed to PWSCC have been identified in the RVCH at CNS-1, MNS-1, and MNS-2. Consequently, the proposed alternative (follow-up at N+3) for these units is more frequent than the N-729-6 Table 1 Item B4.20 requirement, which specifies a maximum volumetric re-examination frequency of every 8 calendar years or before reinspection years (RIY) = 2.25. Since the RIY is less than 2.25 for each RVCH, the proposed alternative of a follow-up volumetric inspection in N+3 is acceptable (three operating cycles at 560°F with an availability factor of 0.95 yields RIY = 1.51). Peening qualified in accordance with the performance criteria of MRP-335 R3-A acts to improve the stress condition of the peened component and reduce PWSCC susceptibility, without introducing adverse effects. Considering that a flaw attributed to PWSCC has been detected at CNS-2, a plant-specific crack growth calculation was performed as reported below to further support the proposed alternative for that unit.

Catawba Unit 2 CRDM Nozzle Axial Crack Growth Calculation

In support of this relief request, a deterministic PWSCC crack growth evaluation (Reference 8.11; also Attachment 1 to this Enclosure) was performed to demonstrate the effectiveness of the proposed alternative to address the potential for PWSCC of CRDM nozzle base metal to lead to pressure boundary leakage at CNS-2. A main objective of the volumetric or surface examinations required under Item B4.20 of ASME Code Case N-729-6, Table 1 is to detect PWSCC degradation affecting the nozzle base metal prior to leakage occurring. As documented in the Attachment to this Enclosure, the crack growth evaluation is specific to the CNS-2 CRDM nozzles, and it applies the same type of deterministic fracture mechanics procedure that has commonly been applied for this purpose. Accordingly, growth of axial flaws originating both on the nozzle outside diameter (OD) centered at the toe of the weld and on the nozzle inside diameter (ID) at the top of the weld was simulated. The crack growth analysis considers the range of geometries and stresses applicable to all CRDM penetrations present on the CNS-2 RVCH.

The initial flaw depth in each case was taken as 10% through the nominal nozzle thickness of 0.625 inch. This common assumption is based on the minimum flaw depth covered by the UT qualification requirements of ASME Code Case N-729-6. Note 13(a) of Table 4-3 of MRP-335 R3-A (Reference 8.1), as conditioned by 10 CFR 50.55a(g)(6)(ii)(D), requires that a volumetric examination of Alloy 600 head penetration nozzles be performed prior to peening mitigation.

Growth of an axial flaw on the nozzle ID was simulated from 10% through the nozzle thickness until the flaw reaches the nozzle OD annulus and causes leakage. Growth of an axial flaw on the nozzle OD centered at the toe of the J-groove weld was simulated from 10% through the nozzle thickness until the upper tip of the flaw reaches the nozzle OD annulus above the weld, causing leakage. These postulated initial locations minimize the flaw growth distance that causes leakage and place the flaw in a region of elevated tensile hoop stress. Each flaw was assumed to have a semi-elliptical shape until penetrating through the nozzle thickness. A reasonably large total-length-to-depth ($2c/a$) aspect ratio of 6 was assumed for the initial flaw in each case. The aspect ratio was permitted to change with time as the crack growth rate was calculated separately for the surface and deepest points on the semi-elliptical crack front according to the stress intensity factors calculated for these two points. The stress intensity factor was determined using the standard influence coefficient approach for a cubic polynomial fit to the total operating condition stress (reflecting weld residual stress and normal operating conditions of pressure and temperature) profile through the nozzle wall thickness. For each case in Reference 8.11 postulating the crack originating on the nozzle OD, the growth calculations showed the crack penetrating to the nozzle ID surface prior to the upper flaw tip reaching the top of the weld and causing leakage. Hence, upon the semi-elliptical flaw penetrating to the ID, the flaw was conservatively modeled to instantaneously transition to an idealized through-wall flaw (extending with rectangular shape through the nozzle thickness) to determine the additional time until the upper tip reaches the top of the weld, resulting in leakage.

Growth was simulated for PWSCC using the standard PWSCC crack growth rate equation of MRP-55 Revision 1 (Reference 8.12), which has been included within Nonmandatory Appendix C of ASME Section XI versions that are incorporated by reference within 10 CFR 50.55a.

The stress profiles applied in the crack growth calculation were determined based on a weld residual stress analysis specifically produced for the CNS-2 CRDM penetrations (Reference 8.13). This analysis applied the industry best practices including simulation of the effect of hydrostatic testing, and the resulting stresses included the effects of normal operating pressure and temperature. The welding was simulated using the best-estimate industry practices for bead size and weld pass location and grouping. For each postulated flaw case for each penetration angle, the most limiting hoop stress profile through the CRDM nozzle wall that results in the shortest time to leakage was identified and conservatively applied in the crack growth evaluation.

For the ID axial flaw case, the most limiting hoop stress profile in the area near or above the top of the weld was selected for each penetration angle. For the OD axial flaw case, both the weld residual stress and weld height (i.e., crack propagation needed to cause leakage) vary around the circumference for non-zero penetration incidence angles. Therefore, for all non-zero penetration incidence angles, the most severe stress profiles from the elevation below the middle of the weld at both the uphill and downhill sides of the nozzle were selected and evaluated as separate cases. These relatively high tensile total stress profiles are conservatively assumed to apply uniformly in the nozzle axial direction despite lower stresses located at and below the weld toe (i.e., the center point for the assumed initial OD flaw). The effect of normal operating pressure on the crack face was appropriately considered in the calculation of stress intensity factor by adding the internal RCS pressure to the membrane stress. Each stress intensity factor applied in the crack growth calculations was conservatively constrained to be no less than 15 MPa√m (13.7 ksi√in) for the entire simulation, ensuring that the stress intensity factor remained well above the stress intensity factor threshold present within the MRP-55 equation. The normal operating temperature applicable to the CNS-2 RVCH of 560°F was applied in the PWSCC crack growth rate equation. Finally, an availability factor of 0.95 was conservatively applied to base the predicted crack growth on operating time in terms of effective full power years (EFPY).

As reported in the attachment, the limiting time for a postulated flaw to grow to cause leakage in the Alloy 600 nozzle is 9.1 calendar years (8.64 EFPY). The limiting case is the time for one of the cases simulating growth of an OD axial crack centered at the toe of the weld to grow from 10% through the nozzle wall until the upper tip of the flaw reaches the annulus at the nozzle OD, causing leakage. In summary, the crack growth evaluation specific to CNS-2 CRDM nozzles shows that the alternative nominal interval of about 4.5 calendar years for volumetric examination of the CRDM penetrations provides reasonable assurance of leak tightness of the Alloy 600 base metal.

The CRDM penetrations including J-groove weld preps at the other CNS and MNS units either have identical or similar design, and all four heads operate at a nominal head temperature no greater than 560°F. Therefore, the CNS-2 crack growth analysis also supports the adequacy of the N+3 examination timing for these other units, which have not reported PWSCC and hence have unmitigated examination interval greater than three cycles.

Effectiveness of Peening for PWSCC Mitigation

Peening mitigation, which prevents future initiation of PWSCC through improvement of the surface stress state, has been performed of each of the 78 CRDM penetrations, vent penetration, and four AHA penetrations at the CNS and MNS RVCHs. Further, the performance criteria in MRP-335 R3-A require demonstration that that peening mitigation does not cause adverse effects. In order to credit the peening mitigation in the inspection requirements for the CRDM and vent penetrations, the peening must be demonstrated to meet the performance criteria of MRP-335 R3-A Section 4.3.8 developed for J-groove welded RVCH penetrations.

Similarly, crediting peening mitigation for the AHA penetrations requires that the peening be demonstrated to meet the performance criteria of MRP-335 R3-A Section 4.2.8 developed for Alloy 82/182 piping butt welds.

The depth of compressive residual stress criterion for the ID of J-groove welded RVCH penetrations is specified as 0.01 inch (0.25 mm) recognizing the limited access for performing peening within the CRDM penetration geometry. As discussed in Section 2.3.2 of MRP-335 R3-A, the effectiveness of a depth of compression of 0.01 inch (0.25 mm) to prevent PWSCC initiation is shown by laboratory and plant experience with peened nickel alloy components. This basis also is applicable to the ID surface of the AHA penetrations. Moreover, inspection of the AHA penetrations is required to include surface examinations, which are especially sensitive to detect shallow PWSCC flaws.

The periodic eddy current (ET) surface examinations of the inside of the AHA penetrations in addition to the UT examination ensures that any existing shallow flaws are detected. Although attached by a butt weld, the AHA head penetrations have a thickness similar to that for CRDM nozzles and diameters similar to that of AHA penetrations at another unit which are attached by a J-groove weld (Reference 8.14), both of which are covered by the performance criteria of Section 4.3.8 MRP-335 R3-A including its minimum depth of compressive residual stress criterion for ID surfaces of 0.01 inch (0.25 mm). There have been no reports to date of any indications attributed to PWSCC that have been detected in AHA penetrations in the U.S. PWR fleet. Thus, as supported by the precedent of the treatment of the ID of the CRDM nozzles in MRP-335 R3-A, the proposed alternative depth of compression on the ID of the AHA penetrations (0.25 mm) will be adequate to ensure the effectiveness of the peening mitigation.

Maintenance of Defense in Depth

Defense in depth is maintained through frequent bare metal visual examinations (VEs) that are performed of the Affected Components and the existing online leakage detection capability. In accordance with MRP-335 R3-A Item B4.50, Duke Energy shall perform a bare metal visual examination of each RVCH penetration nozzle for evidence of pressure boundary leakage every refueling outage. This sensitive visual examination for evidence of pressure boundary leakage will provide defense in depth in the unlikely case that leakage were to occur due to base metal cracking. Similarly, the periodic VEs address the possibility that PWSCC within the Alloy 82/182 J-groove welds could produce leakage resulting in boric acid corrosion. Also, during all refueling outages, IWB-5220 system leakage tests including VT-2 visual examinations and boric acid corrosion control program walkdowns are performed at the periphery of the RVCH.

Moreover, Duke Energy trends RCS leak rate values in accordance with procedures consistent with the guidance of WCAP-16465-NP (Reference 8.15). These guidelines for leak rate monitoring would require a response in the case where the seven-day rolling average of daily RCS unidentified leak rates exceeds 0.1 gallons per minute (gpm), two consecutive days exceed 0.15 gpm, or any day exceeds 0.3 gpm. If an unidentified RCS leak is greater than 1 gpm or if an identified RCS leak is greater than 10 gpm, the plant Technical Specification (TS) 3.4.13, RCS Operational Leakage, outlines the timely actions required to maintain safe operability for recovery, including a shutdown. In addition to periodic RCS leakage calculations, containment radiation detection instrumentation; containment ventilation condensate drain tank level monitors; and containment floor sump level monitors are required to be operable per plant TS 3.4.15, RCS Leakage Detection Instrumentation. These online detection methods ensure that RCS leakage at levels as low as 0.1 gpm would be detected in a timely fashion.

In summary, continued performance of the sensitive VE each refueling outage and online leak detection capabilities maintain defense in depth. Under the proposed alternative, reasonable assurance of structural integrity is provided.

Conclusions:

Approval of the requested alternative to perform the follow-up inspection of the 78 CRDM penetrations and vent penetration at each unit identified in Section 1.0 during the N+3 refueling outage following peening would permit alignment of the timing of the follow-up inspection for all 83 head penetrations at CNS-1, CNS-2, MNS-1, and MNS-2, eliminating hardship concerns including occupational hazards, personnel contamination, and additional radiation exposure from performing two separate inspections at each unit. The savings in dose is estimated to be approximately 250 to 300 mRem per unit considering historical data, but can be higher depending on difficulties experienced that may require additional personnel containment entry.

Duke Energy has determined that the following assessments and supplemental evaluations demonstrate a low probability of RVCH penetration nozzle leakage under the alternative N+3 follow-up examination timing due to Alloy 600 base metal PWSCC. The proposed alternative will ensure structural and leak-tight integrity of the head penetrations, maintaining safety and reliability.

1. The additional cycle for an N+3 inspection has the advantage of allowing more time for potential slow-growing flaws to become more readily detectable during the follow-up inspection.
2. Bare metal visual examinations for evidence of leakage will be performed every refueling outage, providing defense-in-depth to identify leakage through either the J-groove weld or nozzle base metal.
3. The plant-specific deterministic axial crack growth calculation for CNS-2 presented in Attachment 1 of this Enclosure demonstrates that the time for a UT-detectable flaw to grow to cause leakage in the CRDM nozzle base metal is 9.1 calendar years or more than six fuel cycles. Thus, the N+3 follow-up inspection timing gives ample margin against the possibility of a base metal flaw growing to cause leakage between the time of peening and the follow-up inspection, without any crediting of the benefit of peening.
4. The deterministic crack growth results for hypothetical flaws in the Alloy 600 base metal presented within Section 5.2.3.2 of MRP-335 R3-A and in TN-4069-00-01 demonstrate how the N+3 follow-up inspection timing is as effective as the N+2 timing in the case of heads operating at T_{cold} with a nominal 18-month fuel cycle to prevent cracking of a size causing pressure boundary leakage.
5. Without taking credit for the application of peening SSI, the operating experience for unmitigated heads in the U.S. operating at T_{cold} demonstrates how through-wall cracking and leakage due to PWSCC that is detectable by UT examination are unlikely to occur prior to an alternative N+3 inspection.

Furthermore, approval of the proposed alternative depth of compressive residual stress criterion for the AHA penetrations is supported by the precedent of that alternative depth (0.25 mm) being required for the ID of J-groove welded RVCH penetration nozzles. As discussed in Section 2.3.2 of MRP-335 R3-A, the effectiveness of a depth of compression of 0.25 mm to prevent PWSCC initiation is shown by laboratory and plant experience with peened nickel alloy components. Moreover, inspection of the AHA penetrations is required to include surface examinations, which are especially sensitive to detect shallow PWSCC flaws.

Based on foregoing discussion, Duke Energy has determined that the conditions of 10 CFR 50.55a(z)(2) are met in that performing the authorized follow-up inspections for the peened CRDM penetrations and vent penetration in the N+2 refueling outages after peening as specified by 10 CFR 50.55a(g)(6)(ii)(D) and MRP-335 R3-A represents a hardship without a compensating increase in the level of quality and safety. In addition, Duke Energy has determined that the compressive residual stress depth performance criterion of 10 CFR 50.55a(g)(6)(ii)(F) and MRP-335 R3-A in the case of peening mitigation of the AHA penetrations represents a hardship also without a compensating increase in the level of quality and safety. These proposed alternatives will ensure the effectiveness of the peening mitigation, while maintaining safety and reliability.

6.0 DURATION OF PROPOSED ALTERNATIVE:

The proposed Alternative is requested for the remainder of the fourth and through the end of the fifth inspection intervals for CNS-1, CNS-2, and MNS-2 and for the remainder of the fifth inspection interval for MNS-1. The proposed Alternative will not extend beyond the current license period end dates as shown in Table 2.

7.0 PRECEDENTS:

7.1 **ADAMS Accession Number ML19155A060. NRC approval dated June 5, 2019.** Braidwood Station, Unit 1 – Relief from the Requirements of the American Society of Mechanical Engineers Code (EPID L-2018-LLR-0126).

7.2 **ADAMS Accession Number ML19035A294. NRC approval dated February 25, 2019.** Byron Station, Unit No. 2 – Relief from the Requirements of the ASME Code (EPID 2018-LLR-0118).

7.3 **ADAMS Accession Number ML18162A184. NRC approval dated June 4, 2018.** Braidwood Station, Unit 2 – Relief from the Requirements of the American Society of Mechanical Engineers code (EPID L-2017-LLR-0155).

7.4 **ADAMS Accession Number ML23188A043. NRC approval date July 31, 2023.** Millstone Power Station, Unit No. 3 – Authorization and Safety Evaluation for Alternative Request No. IR-4-11 (EPID L-2022-LLR-0067).

7.5 **ADAMS Accession Number ML23256A288. NRC approval date September 20, 2023.** Wolf Creek Generating Station, Unit 1 – Authorization and Safety Evaluation for Alternative Request No. I4R-08 (EPID L-2023-LLR-0010).

8.0 REFERENCES:

8.1 *Materials Reliability Program: Topical Report for Primary Water Stress Corrosion Cracking Mitigation by Surface Stress Improvement (MRP-335, Revision 3-A)*. EPRI, Palo Alto, CA: 2016. 3002009241. [freely available at www.epri.com]

8.2 American Society of Mechanical Engineers Boiler and Pressure Vessel Code (ASME Code) Section XI, *Rules for Inservice Inspection of Nuclear Power Plant Components*, 2007 Edition with the 2008 Addenda.

8.3 ASME Code Case N-729-6, "Alternative Examination Requirements for PWR Reactor Vessel Upper Heads With Nozzles Having Pressure-Retaining Partial-Penetration Welds," Section XI, Division 1, dated March 3, 2016.

8.4 ASME Code Case N-770-5, "Alternative Examination Requirements and Acceptance Standards for Class 1 PWR Piping and Vessel Nozzle Butt Welds Fabricated With UNS N06082 or UNS W86182 Weld Filler Material With or Without Application of Listed Mitigation Activities," Section XI, Division 1, dated November 7, 2016.

8.5 Duke Energy, “Revision to Proposed Alternative to Use Reactor Vessel Head Penetration Embedded Flaw Repair Method,” Relief Request RA-21-0145, dated April 24, 2021. [NRC ADAMS Accession No. ML21114A000]

8.6 Duke Energy, “Proposed Alternative to Use Reactor Vessel Head Penetration Embedded Flaw Repair for Life of Plant,” Relief Request RA-21-0144, dated January 20, 2022. [NRC ADAMS Accession No. ML22020A283]

8.7 U.S. NRC, “Catawba Nuclear Station, Unit 2 – Proposed Alternative Request RA-21-0144 to Use Reactor Vessel Head Penetration Embedded Flaw Repair Method (EPID L-2022-LLR-0010),” dated August 31, 2022. [NRC ADAMS Accession No. ML22213A253]

8.8 Technical Note TN-4069-00-01, Revision 0, “MRP-335 R3-A Matrix of Deterministic Crack Growth Calculations for T_{cold} Reactor Vessel Top Head Nozzles Evaluated for Alternative Peening Follow-up Volumetric Examination Timing,” Dominion Engineering, Inc., Reston, VA August 2018. [NRC ADAMS Accession No. ML18270A066, Attachment 2]

8.9 G. White, K. Fuhr, M. Burkhardt, and C. Harrington, "Deterministic Technical Basis for Re-Examination Interval of Every Second Refueling Outage for PWR Reactor Vessel Heads Operating at T_{cold} with Previously Detected PWSCC," Proceedings of the ASME 2016 Pressure Vessel & Piping Conference, ASME, PVP2016-64032.

8.10 Technical Note TN-4069-00-02, Revision 0, "Experience for Unmitigated CRDM Nozzles in U.S. PWRs Evaluated for Margin Against Leakage Considering Additional PWSCC Growth if Indications Had Remained in Service," Dominion Engineering, Inc., Reston, VA, August 2018. [NRC ADAMS Accession No. ML18270A066, Attachment 3]

8.11 Dominion Engineering, Inc., "Axial Crack Growth Evaluation for CRDM Penetration Nozzles in Catawba Unit 2 RVCH," Non-Proprietary Calculation C-030-2303-00-01, Revision 0, November 2023.

8.12 *Materials Reliability Program (MRP): Crack Growth Rates for Evaluating Primary Water Stress Corrosion Cracking (PWSCC) of Thick-Wall Alloy 600 Materials (MRP-55) Revision 1*, EPRI, Palo Alto, CA: 2002. 1006695. [freely available at www.epri.com]

8.13 Dominion Engineering, Inc., "Catawba Unit 2 Upper Head CRDM Nozzle Welding Residual Stress Analysis," DEI Proprietary Calculation C-3023-00-02, Revision 0, August 2007.

8.14 TVA, "Sequoyah Nuclear Plant, Units 1 and 2, American Society of Mechanical Engineers Boiler and Pressure Vessel Code Section XI, Inservice Inspection Program, Request for Alternative, 18-ISI-1," CNL-19-012, January 30, 2019. [NRC ADAMS Accession No. ML19031C848]

8.15 Westinghouse, "Pressurized Water Reactor Owners Group Standard RCS Leakage Action Levels and Responses Guidelines for Pressurized Water Reactors," WCAP-16465-NP, Revision 0, dated September 2006. [NRC ADAMS Accession No. ML070310082]

Attachment 1 to Enclosure

Dominion Engineering, Inc.

Calculation C-030-2303-00-01, Revision 0

"Axial Crack Growth Evaluation for CRDM Penetration Nozzles in Catawba Unit 2 RVCH"

CALCULATION

Dominion Engineering, Inc.

Title: Axial Crack Growth Evaluation for CRDM Penetration Nozzles in Catawba Unit 2 RVCH

Calculation No.: C-030-2303-00-01 Revision No.: 0

RECORD OF REVISIONS

Rev.	Description	Prepared by Date	Checked by Date	Reviewed by Date	Approved by Date
0	Original Issue	DocuSigned by: 935AD3D8DA444FA... 11/2/2023 T.P. Meurer Engineer	DocuSigned by: D57E192A59494... 11/2/2023 K.J. Fuhr Senior Engineer	DocuSigned by: 56D57E192A59494... 11/2/2023 K.J. Fuhr Senior Engineer	DocuSigned by: 280111486635442... 11/2/2023 G.A. White Principal Engineer

The last revision number to reflect any changes for each section of the calculation is shown in the Table of Contents. The last revision numbers to reflect any changes for tables and figures are shown in the List of Tables and the List of Figures. Changes made in the latest revision, except for Rev. 0 and revisions which change the calculation in its entirety, are indicated by a double line in the right-hand margin as shown here.

NON-PROPRIETARY

TABLE OF CONTENTS

LIST OF TABLES

LIST OF FIGURES

1 PURPOSE

The purpose of this calculation is to document the results of crack growth analyses of control rod drive mechanism (CRDM) penetration nozzles of the reactor vessel closure head (RVCH) in operation at Catawba Nuclear Station, Unit 2 (CNS-2). The analyses calculate the time for a postulated axial flaw in the nozzle tube base metal to grow from an assumed initial size (i.e., 10% through the nozzle nominal wall thickness) until it causes leakage. The 10% through-wall depth corresponds to the minimum crack depth included in the qualification requirements for ultrasonic testing (UT) of CRDM penetrations. As illustrated in Figure 1, in the case of a flaw located on the nozzle inner diameter (ID) surface, leakage is assumed to occur once the flaw penetrates to the nozzle outer diameter (OD) surface. In the case of a flaw located on the nozzle OD surface at the weld toe, leakage is calculated to occur when the flaw grows upward to the nozzle OD annulus above the weld.

The crack growth analysis is performed to determine the number of fuel cycles required for an axial flaw in an unmitigated nozzle tube to grow from a detectable size to cause leakage. This calculation is of relevance to the timing of periodic UT of the nozzle tube for the purpose of addressing the possibility of leakage due to primary water stress corrosion cracking (PWSCC) of the nozzle tube.

2 SUMMARY OF RESULTS

Axial crack growth evaluations were performed applying the specific geometry and loads applicable to CNS-2 CRDM penetration nozzles, including the results of the plant-specific welding residual stress (WRS) analysis documented in DEI Calculation C-3023-00-02, Revision 0 [2] (with the associated full listing of nodal results in DEI Data Disk D-3023-00-02 [3]). Evaluations were performed considering five penetration incidence angles that bound the range of incidence angles of the CNS-2 CRDM penetration nozzles: 0°, 16.2°, 26.2°, 36.3°, and 48.7°. The results of the crack growth calculations for the limiting ID nozzle surface flaw and the limiting OD nozzle surface flaw across the range of penetration angles and locations (uphill or downhill side of nozzle) are provided in Table 4 and Table 5, respectively.

The overall limiting case is for a flaw originating on the nozzle OD surface at the uphill toe of the J-groove weld in a penetration with an incidence angle of 16.2°. A crack growth time of 9.1 calendar years (8.64 EFPY) from a crack with detectable depth until leakage is calculated for this case. The limiting crack growth time for a flaw originating on the nozzle ID surface is 18.6 calendar years (17.7

EFPY). The results of these crack growth calculations demonstrate reasonable assurance that leak tightness will be maintained for the nozzle base metal of the CRDM penetrations beyond six operating cycles.

3 INPUT REQUIREMENTS

The following inputs are used for the analysis supporting this calculation:

1. The nominal geometry of the RVCH and CRDM penetrations is provided in Reference [2]. The relevant dimensions of the CRDM penetrations and J-groove welds are as follows:
   a. Nozzle:
   - CRDM Nozzle OD = 4.00 inches
   - CRDM Nozzle ID = 2.75 inches
   - CRDM Nozzle thickness, t = (4.00 – 2.75)/2 = 0.625 inch
   - CRDM Nozzle incidence angles:
     i) 0° (Penetration No. 1)
     ii) 16.2° (Penetration Nos. 6 through 9)
     iii) 26.2° (Penetration Nos. 22 through 29)
     iv) 36.3° (Penetration Nos. 50 through 53)
     v) 48.7° (Penetration Nos. 74 through 78)

   b. J-groove weld height specific to CRDM penetrations with incidence angles defined in Input 1.a are calculated from the axial heights documented in Tables 4, 6, 8, 10, and 12 and the nodal location information shown in Figure 3 of [2] and provided in Table 1.
2. The operating conditions for the CNS Unit 2 RVCH are as follows:
   a. Operating Pressure: 2250 psia [4]
   b. Operating Temperature: 560°F [5]
3. The operating stress profiles (including welding residual stress) for the CNS-2 CRDM Penetrations are calculated by finite-element analysis (FEA) in DEI Calculation C-3023-00-02 R0 [2]. That analysis considers the local configurations of the J-groove weld attaching the CRDM penetration nozzles to the RVCH. DEI Data Disk D-3023-00-02 R0 [3] tabulates the total hoop stress during operation for all nodes in the FEA model, including the Alloy 600 CRDM nozzle base material. Key nodal results from [3] that are applied in this calculation are presented in Table 2 of this calculation.[1]

[1] An operating temperature of 557°F is applied in the FEA models of Reference [2]. The difference in stresses between a normal operating temperature of 560°F and 557°F is negligible.

4. The material of construction for the CRDM nozzles in the CNS-2 RVCH is Alloy 600 [6]. The J-groove weld for the CRDM penetrations is formed using Alloy 82 and/or Alloy 182 material [6].
5. The PWSCC crack growth rate for Alloy 600 is per C-8511 from Nonmandatory Appendix C of ASME Section XI [8]. The cited 2019 Edition of ASME Section XI is incorporated by reference within the NRC regulations (10 CFR 50.55a). The PWSCC crack growth rate equation in Reference [8] is identical to that published in MRP-55 [7] for thick-wall wrought Alloy 600 material.
6. The stress intensity factor (K_I) of hypothetical cracks in the CRDM nozzle are obtained using the influence coefficient method in the French RSE-M and RCC-MR code appendices for flaw analysis, as documented by Marie et al. [9]. This approach is applied using the appropriate tabular coefficients developed for cylindrical pipes:
    a. For the semielliptical flaw on the inside surface of the nozzle tube, the coefficients are per TUB-LDSI (Table 39) [9].
    b. For the semielliptical flaw on the outside surface of the nozzle tube, the coefficients are per TUB-LDSE (Table 44) [9].
    c. For the idealized flaw through the nozzle thickness assumed upon penetration of the OD surface flaw to the nozzle ID, the coefficients are per TUB-LTR (Table 35) [9].
7. Given the CRDM penetration geometry ([2] and Input 1), as illustrated in Figure 1, pressure boundary leakage will occur if either of the following conditions develop:
    a. For an axial flaw growing from the nozzle inside surface at or above the weld, leakage would occur once the flaw depth reaches 100% of the nozzle wall thickness.
    b. For an axial flaw growing from the nozzle wetted outside surface at or below the weld toe, leakage would occur once the upper crack tip reaches the OD nozzle annulus (i.e., at the elevation of the J-groove weld root).

4 ASSUMPTIONS

1. This calculation considers axial flaws in the CRDM nozzle tube (i.e., flaws that are detectable during periodic volumetric examinations before they grow to cause leakage). The limiting locations that are considered are a flaw centered on the nozzle outer surface at the bottom (toe) of the J-groove weld and a flaw on the nozzle inner surface near or above the top of weld elevation. Flaws at these two locations have the shortest distance to grow to cause leakage and are subject to highly tensile stress profiles. As shown in C-3023-00-02 R0 [2], the axial stresses that would drive circumferential crack growth are much less tensile in magnitude than the corresponding hoop stresses and remain below 56 ksi at all locations. Hence, the axial flaw results bound the time for growth of circumferential flaws.
2. The end condition for this crack growth evaluation is the occurrence of leakage (see Input 7).

3. In accordance with the common practice for calculating crack-tip stress intensity factors (e.g. per Nonmandatory Appendix A of ASME Section XI [10], or as documented in Marie et al. [9]), axial surface flaws evaluated in this crack growth calculation are modeled to have a semielliptical shape.

4. For the case analyzing the outside surface flaw, it is assumed that when the crack grows to 100% depth ($a = t$) and penetrates to the nozzle ID surface, the crack transitions immediately from semielliptical shape to an idealized, uniform-length slit extending through the nozzle thickness. The initial length of the idealized through-the-nozzle-thickness flaw is taken as the length (i.e., axial extent) of the semielliptical flaw when it penetrates to the nozzle ID. This is a conservative assumption that neglects the time over which the transition occurs.

5. An initial aspect ratio ($2c/a$) of 6 is conservatively applied, as longer flaws tend to have higher stress intensity factors at the crack tip on both the surface and the deepest points, and thus grow more rapidly. The aspect ratio evolves over time due to the differing growth rates calculated at the surface tip and deepest point of the crack.

6. An initial flaw depth of 10% through the nozzle wall thickness ($a/t = 0.1$) is applied, which is the minimum flaw depth covered by the ultrasonic testing (UT) qualification requirements of ASME Code Case N-729-6 [11]. Note 13(a) of Table 4-3 of MRP-335 R3-A [1], as conditioned by 10 CFR 50.55a(g)(6)(ii)(D), requires that a volumetric examination of Alloy 600 head penetration nozzles be performed prior to peening mitigation. Further, Note 13(e) of Table 4-3 of MRP-335 R3-A requires that flaws detected during the pre-mitigation inspection shall be corrected by a repair or replacement activity. Hence, it is conservative to postulate that a surface-connected planar flaw of 10% through-wall depth would be present at the start of head operation immediately following peening mitigation.

7. As stated in MRP-55 [7], the laboratory data used to develop the MRP-55 crack growth rate equation did not include stress intensity factor values below about 15 MPa√m (13.65 ksi√in). Hence, each stress intensity factor used for calculating the crack growth rate will be conservatively selected as the maximum of the value calculated by Equation [5-1] and 15 MPa√m (13.65 ksi√in), ensuring that the stress intensity factor threshold (K_{th}) of the MRP-55 equation, which was implemented in Section XI as C-8511, is not given inappropriate weight.

8. As the augmented examination requirements per ASME Code Case N-729-6 [11] were developed to address the potential for PWSCC degradation of the RVCH penetrations, this analysis considers crack growth due to PWSCC. Growth due to fatigue of the postulated flaws is not considered.

9. Consistent with the required inputs for the influence coefficient method approach [9], a third-order polynomial is used to fit the stress profile driving growth for the part-depth flaws.

10. The operating stress profiles (including welding residual stress) extracted from the FEA results correspond to the elevations with elevated tensile hoop stresses that result in the fastest growth to leakage for each postulated flaw location (Assumption 1):

a. The stress profile for the inside surface flaw is conservatively taken from the nodes at the uphill side of the nozzle at the "top of weld" elevation (defined in C-3023-00-02 R0 [2]) for all penetration angles except the 48.7° case. The uphill side, "top of weld" elevation is the limiting elevation and circumferential location in the region near or above the top of the weld that results in the fastest ID flaw growth beginning with $a/t = 0.1$ until penetration to the nozzle OD ($a = t$) and assumed leakage. For the 48.7° case, crack growth calculations are performed for the "top of weld" stress profiles at both the uphill and downhill sides of the nozzle, as neither profile is clearly limiting. The nodal hoop stress results from C-3023-00-02 R0 [2] for these limiting locations are tabulated in Table 2 of the current calculation.

b. For the outside surface flaw case, crack growth calculations are performed using stress profiles taken from both the uphill and downhill sides of the nozzle for each penetration angle, as these are the two circumferential positions with potentially limiting stress profiles. A single profile is applied for the 0° penetration angle, since that is an axisymmetric geometry. As defined in C-3023-00-02 R0 [2], the weld extends upward in increments of 100 from the 600- to the 1400-series nodal row, with the uphill nodes starting from 120000. For the downhill side of each nozzle, the stress profile is conservatively taken from the nodes one row above the "bottom of weld" elevation (i.e., the 700-series tube nodes), which yield the most severe (i.e., the shortest time to leakage) stress profiles on the downhill side. For the uphill side, the more severe stress profile at the elevation one or two nodal rows below the "middle of weld" elevation (i.e., the 120800- or 120900-series tube nodes) is taken. These profiles are taken from the detailed results archived in D-3023-00-02 R0 [3] and are tabulated in Table 2 of the current calculation.

c. The single hoop stress applied for the growth of idealized through-the-nozzle-thickness flaws is taken as the average of the polynomial hoop stress profile defined above that is applied for part-depth flaw growth.

11. Values for the influence coefficients are obtained by interpolating or extrapolating from tables in Marie et al. [9]. Coefficients are provided for $0.0625 \leq a/c \leq 1.0$ and $0 \leq a/t \leq 0.8$.

a. For input parameters inside the domains provided inside those tables, influence coefficients are determined through log-linear interpolation on t/R_i and on a/c, and linear interpolation on a/t.

b. The only time input parameters are required outside of the provided domains is for the crack growth beyond $a/t > 0.8$. Therefore, the influence coefficients are linearly extrapolated for the range $0.8 < a/t < 1.0$. Extrapolation of influence coefficients for $a/t > 0.8$ is necessary to calculate the time until leakage and common practice (e.g., [12]).

12. Time steps of 0.025 year (for the part-depth outside surface flaw), 0.01 year (for the idealized through-the-nozzle-thickness flaw), and 0.05 year (for the inside surface flaw) are applied for the crack growth calculations. These time steps are appropriately refined to yield converged results given the timescale over which a crack in Alloy 600 grows to the nozzle OD annulus and causes leakage.

13. A capacity factor characteristic of future operation of 0.95, corresponding to an outage duration of 27 days for each 18-month fuel cycle ((1-0.95)×365.25×1.5=27.4), is conservatively assumed. Thus, the effective full power years (EFPY) corresponding to each future calendar year of operation is 0.95 EFPY.

5 ANALYSIS

This calculation document describes the stress intensity factor calculations (Section 5.1) and crack growth calculations (Section 5.2) performed specific to the CRDM penetration nozzles of the RVCH at CNS-2. Deterministic crack growth calculations are used to determine the time required for a postulated axial flaw to grow from an initial depth of 10% through the nozzle thickness to leakage. Growth of an axial flaw on the nozzle ID is simulated until the flaw reaches the nozzle OD annulus and causes leakage. Growth of an axial flaw on the nozzle OD centered at the toe of the J-groove weld is simulated until the upper tip of the flaw reaches the nozzle OD annulus above the weld, causing leakage. These postulated initial locations minimize the flaw growth distance that causes leakage and place the flaw in a region of elevated tensile hoop stress. Crack growth calculations are performed applying stresses and geometries for five nozzle penetration angles, 0°, 16.2°, 26.2°, 36.3° and 48.7°, which represent and bracket the range of nozzle penetration angles for the CNS-2 RVCH.

5.1 Stress Intensity Factor Calculation

5.1.1 Loads and Stresses

Tensile stresses are one of the key factors influencing PWSCC. For the purposes of crack growth calculations, only stresses orthogonal to the plane of crack growth are considered (i.e., only stresses in the hoop direction drive axial crack growth). The stresses that drive PWSCC growth are the welding residual stresses and normal operating stresses that are present during steady-state operation.

As described in Input 3, welding residual stresses and normal operating stresses were calculated using finite-element analyses that are documented in DEI Calculation C-3023-00-02 R0 [2], with the full set of detailed nodal results archived in DEI Data Disk D-3023-00-02 [3]. That analysis considers the local configuration of the J-groove weld attaching the CRDM Penetration nozzles to the RVCH for the range of penetration angles at Catawba 2. Key nodal results relevant to this crack growth calculation are repeated in Table 2 of this calculation. The hoop stress profiles that are selected for the crack growth analyses for ID- and OD-surface flaws are plotted as points in Figure 2 and Figure 3, respectively, as a function of relative distance through the nozzle tube. Figure 2 and Figure 3 also show cubic fits to the nodal stresses, with the fitted coefficients documented in Table 3. The stress profiles corresponding to the limiting ID and OD postulated flaw cases are plotted in Figure 4.

Due to stresses from nozzle ovalization, for non-zero penetration angles, the most tensile hoop stress profile occurs at either the “uphill” (closest to the top of the head) or “downhill” side of the nozzle rather than one of the intermediate “sidehill” circumferential positions. Where one of the stress profiles at either the uphill or downhill sides of the nozzle is not clearly the more severe, both of these potentially bounding locations are selected.

The stress profile for the inside surface flaw case is taken from the nodes at the “top of weld” elevation, which is the limiting elevation in the region near or above the top of the weld that results in the fastest ID flaw growth beginning with $a/t = 0.1$ until penetration to the nozzle OD ($a = t$) and assumed leakage.

For the outside surface flaw case, both the weld residual stress and weld height (i.e., crack propagation needed to cause leakage) vary around the circumference for non-zero penetration angles. Therefore, for all non-zero penetration angles, stress profiles at both the uphill and downhill sides of the nozzle are selected. The stress profile for the outside surface flaw on the downhill side of each nozzle is taken at one nodal row above the bottom toe of the weld, which has the most severe weld residual stresses of all downhill side elevations. The stress profile for the outside surface flaw on the uphill side of each nozzle is taken at one or two nodal rows below the middle of the weld (i.e., the midpoint between the weld toe and top of the weld), as the most severe elevation varies with penetration angle. These relatively high tensile total stress profiles are conservatively assumed to apply uniformly in the nozzle axial direction despite lower stresses at and below the weld toe (i.e., the center point for the assumed initial flaw).

A membrane stress equal in value to the operating pressure, P, is also included in the crack growth analysis to properly account for the additional stress resulting from application of the internal pressure, P, to the crack face. The superposition principle of linear elastic fracture mechanics (LEFM) allows treatment of the crack face pressure as a remote membrane stress loading.

5.1.2 Influence Coefficient Method

Given the total hoop stress profiles defined in Section 5.1.1, along with the assumed initial depth and aspect ratio of the crack (Assumptions 5 and 6), stress intensity factors are calculated using the influence coefficient method. Figure 2 and Figure 3 show the cubic fit (3rd order polynomial) to the hoop stress distributions for use with the influence coefficient method (Assumption 9), and Table 3 lists the coefficients resulting from the polynomial fit.

For axial semielliptical part-depth cracks, the general form of the mode I stress intensity factor calculation by way of the influence coefficient method is provided by Marie et al. [9] for a cylindrical pipe geometry:

$$K_{\mathrm{I}} = \sqrt{\pi a} \sum_{j=0}^{3} i_j \left(\frac{t}{R_i}, \frac{a}{c}, \frac{a}{t} \right) \cdot \sigma_j \cdot \left[\frac{a}{t} \right]^j \qquad [5\text{-}1]$$

where:

K_{I} = mode I stress intensity factor (ksi√in)

i_j = coefficient of influence of order j (function of geometry of crack and nozzle)

a = crack depth from the flawed surface (in.)

c = crack half-length (in.)

t = CRDM nozzle thickness (in.)

R_i = CRDM nozzle inner radius (in.)

σ_j = coefficient of order j of polynomial fit stress profile as function of x/t (ksi)[2]

[2] The σ_0 is the sum of the 0th order polynomial coefficient and the internal pressure to account for the influence of crack face pressure on the stress intensity factor.

Different tabular values for i_j per the tables listed in Input 6 are applied when calculating K_I for the surface tip ($K_{I,0}$) and the deepest tip ($K_{I,90}$) of the flaw [9]. Values from tables of influence coefficients are interpolated in t/R_i, a/c, and a/t to obtain values of i_j specific to the crack geometry at a given timestep. This is accomplished by performing interpolation of the influence coefficients (Assumption 11):

1. Log-linear interpolation in t/R_i (i.e., linear interpolation of values on the scale $\ln(t/R_i)$)
2. Log-linear interpolation in a/c
3. Linear interpolation in a/t
   a. If $a/t > 0.8$, linearly extrapolate up to $a/t = 1.0$ (Assumption 11.b).

For axial through-the-nozzle-thickness cracks loaded by a remote membrane stress, the general form of the mode I stress intensity factor calculation by way of the influence coefficient method is provided by Marie et al. [9] for a cylindrical pipe geometry:

$$K_I = \sigma_m F_m(\lambda)\sqrt{\pi c} \quad [5\text{-}2]$$

where:

K_I = mode I stress intensity factor (ksi√in)
c = crack half-length (in.)
σ_m = remote membrane stress (ksi) (per Assumption 10.c and including crack face pressure)
F_m = influence coefficient for membrane stress (function of geometry parameter λ)
λ = $c/\sqrt{R_m t}$
R_m = mean radius of nozzle (in.)

Interpolation is applied to obtain F_m as a function of the current value of λ.

5.2 Crack Growth Calculation

5.2.1 Approach

As discussed in Input 5, the crack growth analysis applies the PWSCC crack growth rate for Alloy 600. Accordingly, the standard PWSCC crack growth rate equation described in ASME Section XI Nonmandatory Appendix C [8] for Alloy 600 is applied:

$$\frac{da}{dt} = \exp\left[-\frac{Q_g}{R}\left(\frac{1}{T} - \frac{1}{T_{\text{ref}}}\right)\right]\varphi(K_{\text{I},90} - K_{th})^{\eta} \quad [5\text{-}3]$$

$$\frac{dc}{dt} = \exp\left[-\frac{Q_g}{R}\left(\frac{1}{T} - \frac{1}{T_{\text{ref}}}\right)\right]\varphi(K_{\text{I},0} - K_{th})^{\eta} \quad [5\text{-}4]$$

where

- da/dt = crack growth rate at the deepest point of the crack (in/hr)
- dc/dt = crack growth rate at each surface point of the crack (in/hr)
- Q_g = thermal activation energy for crack growth = 31.0 kcal/mol [8]
- R = universal gas constant = 1.103×10^{-3} kcal/(mol-°R)
- T = absolute operating temperature at crack location = 1019.67°R (Input 2.b)
- T_{ref} = absolute temperature (617°F) used to normalize crack growth data = 1076.67°R [8]
- φ = crack growth rate coefficient for Alloy 600 = 4.21×10^{-7} (in/hr)(ksi√in)$^{-\eta}$ [8]
- $K_{\text{I},90}$ = stress intensity factor at the deepest point of the crack, calculated per Section 5.1 (ksi√in)
- $K_{\text{I},0}$ = stress intensity factor at the surface point of the crack, calculated per Section 5.1 (ksi√in)
- K_{th} = threshold stress intensity factor for stress corrosion cracking = 8.19 ksi√in [8]
- η = crack growth rate exponent = 1.16 [8]

The stress intensity factor K_{I} used for calculating the crack growth rate was conservatively constrained to be no less than 15 MPa√m (13.65 ksi√in) as discussed in Assumption 7.

To model growth of the cracks over time, the crack growth rate is calculated and integrated using a fully explicit forward-difference approximation to determine the new crack depth and length using the time steps stated in Assumption 12. Using this approach, the times required for the flaw growth to reach the end condition of leakage (Input 7) are calculated.

Initial conditions applied assume an initial crack depth of 10% through the nozzle thickness (Assumption 6), along with an initial aspect ratio ($2c/a$) of 6 (Assumption 5). As discussed in Section 5.1.1, appropriately conservative hoop stress profiles are applied in the evaluation for each assumed flaw location (Assumption 10; Figure 2, Figure 3).

5.2.2 Results

The times required for a flaw with an initial depth of 10% through the nozzle thickness to grow to a size causing leakage in Alloy 600 are reported in Table 4 for ID-surface flaws and in Table 5 for OD-surface flaws. Initial axial flaws located on both the ID and OD wetted nozzle surfaces were evaluated to determine the limiting case for the time until pressure boundary leakage occurs. The ID flaw case is for a flaw located near or above the top of the weld, where leakage would occur immediately or shortly after the flaw penetrates to the nozzle OD surface. The OD flaw case is for an initial flaw centered at the weld bottom (i.e., weld toe location), with leakage resulting when the half-length (c) of the flaw reaches the value of the weld height along the nozzle OD. Both ID and OD flaw cases were evaluated for five penetration angles, 0°, 16.2°, 26.2°, 36.3° and 48.7°, which represent and bound the range of nozzle penetration angles for the CNS-2 RVCH.

The overall limiting case is the time for an OD axial crack centered at the toe of the weld to grow from 10% through the nozzle thickness until the upper tip of the flaw reaches the annulus at the nozzle OD. As shown in Table 5, the limiting time for a postulated flaw to grow to cause leakage in the Alloy 600 material is 8.64 EFPY (9.1 calendar years), which is calculated for the 16.2° penetration angle using the uphill side stress profile. The limiting time for an inside surface flaw to grow to cause leakage is 17.7 EFPY (18.6 calendar years), which is calculated for the 48.7° penetration angle applying the downhill side stress profile.

Figure 5 through Figure 10 plot key results for the limiting ID and OD flaw cases, which are the 48.7°, downhill case for an ID flaw and the 16.2°, uphill case for an OD flaw. Figure 5 and Figure 6 show the stress intensity factor as a function of time for both inside and outside flaws at the deepest point and the surface point of the crack, respectively. Figure 7 and Figure 8 show the growth in time of crack depth and crack length, respectively, while Figure 9 and Figure 10 show the crack aspect ratio evolution as a function of crack depth and crack length, respectively.

5.3 Software Usage

The following software, controlled in accordance with DEI's quality assurance program for nuclear safety-related work [13], was used in preparing this calculation.

The stress intensity factor and crack growth calculations used in this work were performed using Excel for Office 365 Version 2308 as a one-time-use spreadsheet on a Dell Precision 5570 with an Intel(R) Core(TM) i7-12800H processor and running Windows 11 Enterprise 22H2 (Build 22621.2134).

The results from this one-time-use spreadsheet were checked and reviewed in accordance with DEI's Nuclear Quality Assurance program ([13], [14]). As discussed in M-030-2303-00-01 R0 [15], an alternate calculation implementing the same methodology was used to validate the results. This alternate calculation was prepared independently of the original calculation to be checked. Native electronic files for the spreadsheet calculation and the alternate calculation are included in data disk D-030-2303-00-01 R0 [16], the contents of which are listed for convenience in Appendix A.

6 REFERENCES

1. *Materials Reliability Program: Topical Report for Primary Water Stress Corrosion Cracking Mitigation by Surface Stress Improvement (MRP-335 Revision 3-A)*, EPRI, Palo Alto, CA: 2016. 3002009241. [freely available at https://www.epri.com]
2. Dominion Engineering, Inc., "Catawba Unit 2 Upper Head CRDM Nozzle Welding Residual Stress Analysis," DEI Proprietary Calculation C-3023-00-02, Revision. 0, August 2007.
3. Dominion Engineering, Inc., Data Disk D-3023-00-02, Revision 0. August 2007.
4. Duke Energy, "Chapter 5 – Reactor Coolant System and Connected Systems," *Catawba Nuclear Station UFSAR*, Version of October 9, 2019. NRC ADAMS Accession Number ML20106E914.
5. Duke Energy, Technical Requirements Document CNR-2201.01-00-0007, Rev. 1, "Technical Basis for RVCH Post-Peening NDE Relief Request," May 2023.
6. Letter from Catawba Nuclear Station to U.S. NRC, Request for Alternative RA-21-0144, "Proposed Alternative to Use Reactor Vessel Head Penetration Embedded Flaw Repair for Life of Plant," dated January 20, 2022. NRC ADAMS Accession Number ML22020A283.

7. *Materials Reliability Program (MRP): Crack Growth Rates for Evaluating Primary Water Stress Corrosion Cracking (PWSCC) of Thick-Wall Alloy 600 Materials (MRP-55) Revision 1*, EPRI, Palo Alto, CA: 2002. 1006695. [freely available at https://www.epri.com]
8. ASME Boiler and Pressure Vessel Code, Section XI, Division 1, Nonmandatory Appendix C, "Analytical Evaluation of Flaws in Piping," 2019 Edition.
9. S. Marie et al., "French RSE-M and RCC-MR code appendices for flaw analysis: Presentation of the fracture parameters calculation—Part III: Cracked pipes," *International Journal of Pressure Vessels and Piping*, Vol. 84, pp. 614-658, 2007.
10. ASME Boiler and Pressure Vessel Code, Section XI, Division 1, Nonmandatory Appendix A, "Analytical Evaluation of Flaws," 2019 Edition.
11. ASME Boiler and Pressure Vessel Code Case N-729-6, Alternative Examination Requirements for PWR Reactor Vessel Upper Heads With Nozzles Having Pressure-Retaining Partial-Penetration Welds, Section XI, Division 1, approval date March 3, 2016.
12. D. Rudland, D.-J. Shim, and S. Xu, "Simulating Natural Axial Crack Growth in Dissimilar Metal Welds due to Primary Water Stress Corrosion Cracking," *Proceedings of ASME 2013 Pressure Vessels and Piping Conference*, July 14-18, 2013, Paris, France, ASME, 2013. PVP2013-97188.
13. Dominion Engineering, Inc., *Quality Assurance Manual for Safety-Related Nuclear Work*, DEI-002, Revision 18, November 2010.
14. Dominion Engineering, Inc., *Control of Analyses/Calculations*, QAP-1008-06-302, Revision 3, January 2012.
15. Dominion Engineering, Inc., "Verification of One-Time-Use Spreadsheet Outputs for C-030-2303-00-01 R0," Memo M-030-2303-00-01, Revision 0, November 2023.
16. Dominion Engineering, Inc., Data Disk D-030-2303-00-01, Revision 0, November 2023.

Table 1. Weld Heights for Each Penetration Incidence Angle

Penetration Incidence Angle (°)	Weld Height – Downhill Side (in.)	Weld Height – Uphill Side (in.)
0	1.00	1.00
16.2	1.05	0.96
26.2	1.16	1.08
36.3	1.21	1.20
48.7	1.41	1.45

Table 2. Limiting Hoop Stress Profiles for ID- and OD-initiated Cracking [3]

Stress Profile	Penetration Angle (°)	Profile Location	Hoop Stress (psi), for Given Distance Through Nozzle Wall*					
			0%	20%	40%	60%	80%	100%
Inside	0	Top of weld**	27654	26097	28840	35249	42076	22963
	16.2	Uphill side, top of weld	34421	31785	34339	38646	45609	47117
	26.2	Uphill side, top of weld	37416	34256	36807	40060	46604	51421
	36.3	Uphill side, top of weld	39588	36941	39643	40886	44203	51239
	48.7	Uphill side, top of weld	37532	35629	39218	39106	36595	39822
		Downhill side, top of weld	42916	41360	40663	41773	33941	6631
Outside	0	1 nodal row above bottom of weld**	16296	17921	21635	33602	57123	72172
	16.2	Uphill side, 2 nodal rows below middle of weld	14380	20955	30466	45331	64002	75313
		Downhill side, 1 nodal row above bottom of weld	13196	17021	23206	35327	57655	77085
	26.2	Uphill side, 1 nodal row below middle of weld	24104	27490	36244	49181	64374	70946
		Downhill side, 1 nodal row above bottom of weld	13542	17817	24912	38271	60169	80382
	36.3	Uphill side, 1 nodal row below middle of weld	33076	35163	43904	55179	66400	67658
		Downhill side, 1 nodal row above bottom of weld	11244	17645	27731	42693	64999	87936
	48.7	Uphill side, 1 nodal row below middle of weld	43233	44456	51756	58457	64119	64156
		Downhill side, 1 nodal row above bottom of weld	6975.1	17030	31266	48795	71829	91731

* Stresses are presented as a function of relative distance from the nozzle ID (0%) to the nozzle OD (100%).

** The WRS profiles for the 0° penetration angle are uniform around the circumference, and therefore, the tabulated profile represents both the uphill and downhill sides of the nozzle.

Table 3. Cubic Stress Profile Fit to Limiting Hoop Stress WRS Profiles

Stress Profile	Penetration Angle (°)	Profile Location	Coefficients of Polynomial Fit of Stress Profile (psi), originating from flawed surface**				Average Stress* (psi)
			σ_3	σ_2	σ_1	σ_0 *	
Inside	0	Top of weld	-186278	247522	-65773	28491	Not Used***
	16.2	Uphill side, top of weld	-58468	104825	-33555	34535	
	26.2	Uphill side, top of weld	-34054	76018	27838	37356	
	36.3	Uphill side, top of weld	2834	18460	-9547	39238	
	48.7	Uphill side, top of weld	5944	-8359	4733	36899	
		Downhill side, top of weld	-155014	162293	-43659	43373	
Outside	0	1 nodal row above bottom of weld	49655	-9149	-96545	73189	34280
	16.2	Uphill side, 2 nodal rows below middle of weld	64958	-70509	-55427	75821	40844
		Downhill side, 1 nodal row above bottom of weld	15598	40262	-119893	77752	35126
	26.2	Uphill side, 1 nodal row below middle of weld	87646	-112859	-21694	71325	44770
		Downhill side, 1 nodal row above bottom of weld	18171	34753	-119854	80915	37115
	36.3	Uphill side, 1 nodal row below middle of weld	105149	-155146	15344	67900	50144
		Downhill side, 1 nodal row above bottom of weld	9104	45076	-130955	88260	40084
	48.7	Uphill side, 1 nodal row below middle of weld	69248	-109444	19191	64123	54549
		Downhill side, 1 nodal row above bottom of weld	34641	-14270	-105237	92063	43348

* These stresses do not include the effect of crack face pressure.

** Stress profiles are fitted as a function of relative radial distance from the initiating surface (x), i.e., the stress profile is from $x = 0$ at the outer surface to $x = 1$ at the inner surface for the "Outside" stress profile.

*** ID flaw growth calculations do not include idealized through-the-nozzle-thickness flaw growth, so average stress is not used.

Table 4. Crack Growth Results – ID-Initiated Surface Flaw

Penetration Angle (°)	WRS Profile	Total Growth Time to Leakage (EFPY)
0	Top of weld	34.78
16.2	Uphill side, top of weld	24.11
26.2	Uphill side, top of weld	21.14
36.3	Uphill side, top of weld	18.95
48.7	Uphill side, top of weld	20.24
	Downhill side, top of weld	17.71

Table 5. Crack Growth Results – OD-Initiated Surface Flaw

Penetration Angle (°)	WRS Profile	Growth Time to Idealized Through-the-Nozzle-Thickness Flaw (EFPY)	Total Growth Time to Leakage (EFPY)
0	1 nodal row above bottom of weld	10.07	10.12
16.2	Uphill side, 2 nodal rows below middle of weld	8.55	8.64
	Downhill side, 1 nodal row above bottom of weld	9.53	9.84
26.2	Uphill side, 1 nodal row below middle of weld	8.47	9.33
	Downhill side, 1 nodal row above bottom of weld	8.92	9.81
36.3	Uphill side, 1 nodal row below middle of weld	8.14	9.53
	Downhill side, 1 nodal row above bottom of weld	7.94	8.96
48.7	Uphill side, 1 nodal row below middle of weld	8.22	10.32
	Downhill side, 1 nodal row above bottom of weld	7.17	8.83

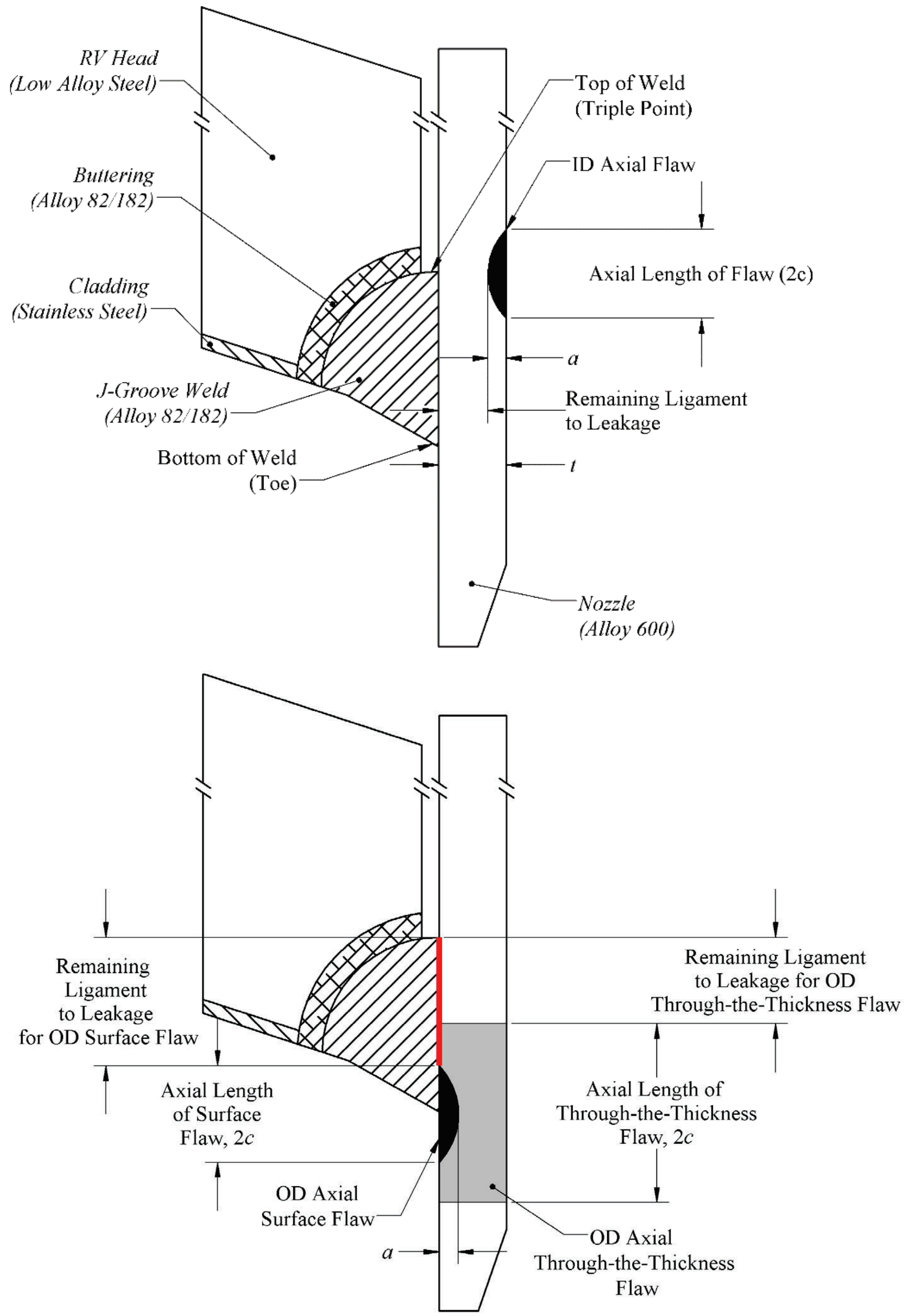

Figure 1. Hypothetical Flaw Growth Geometry Definition

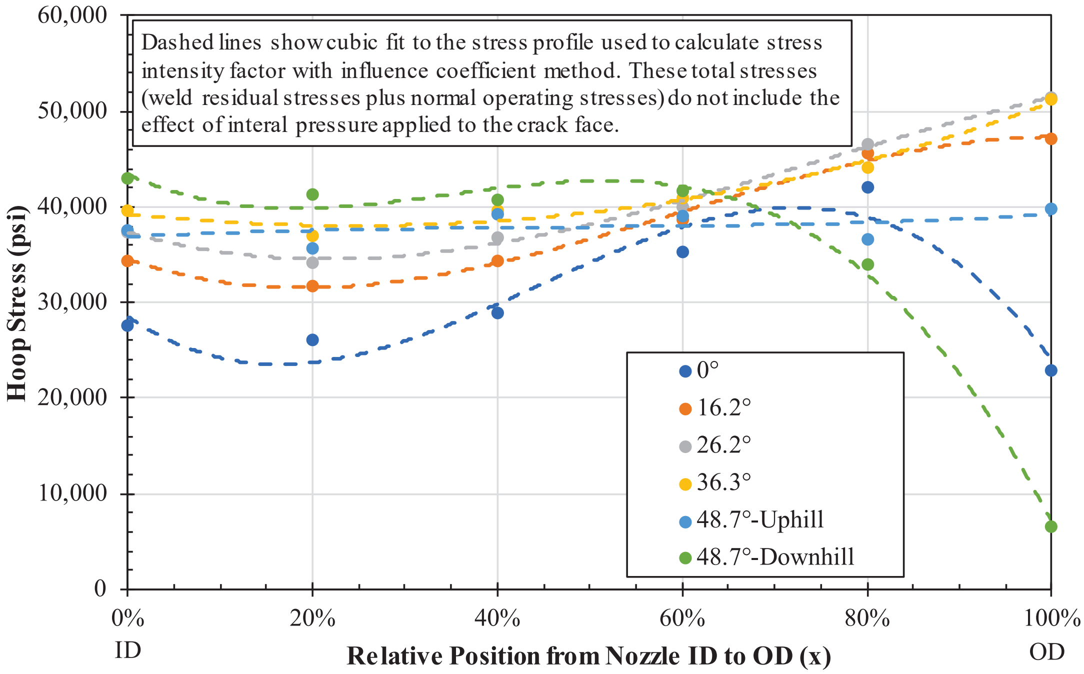

Figure 2. Total Stress Profiles Applied in Crack Growth Evaluation ID-Surface Flaw Cases

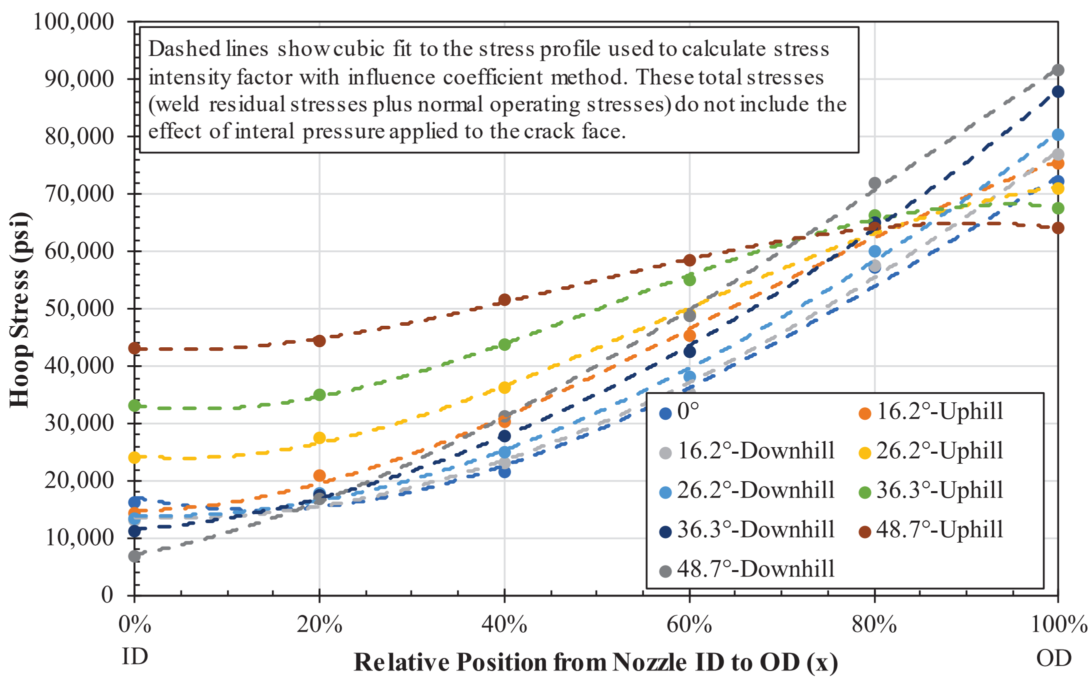

Figure 3. Total Stress Profiles Applied in Crack Growth Evaluation OD-Surface Flaw Cases

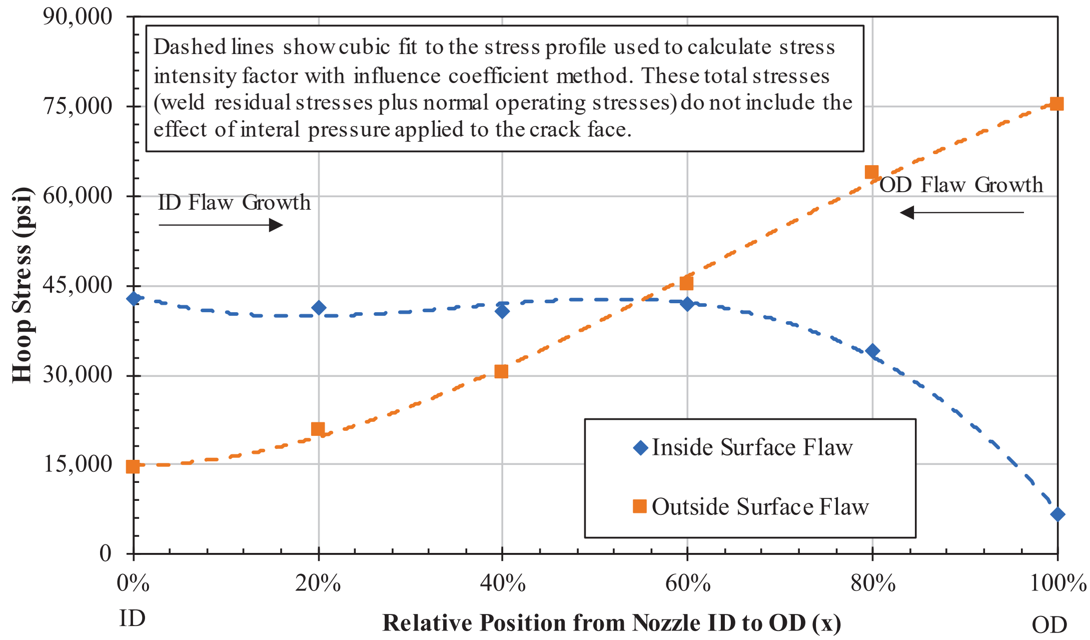

Figure 4. Limiting Total Stress Profiles Applied in Crack Growth Evaluation Cases

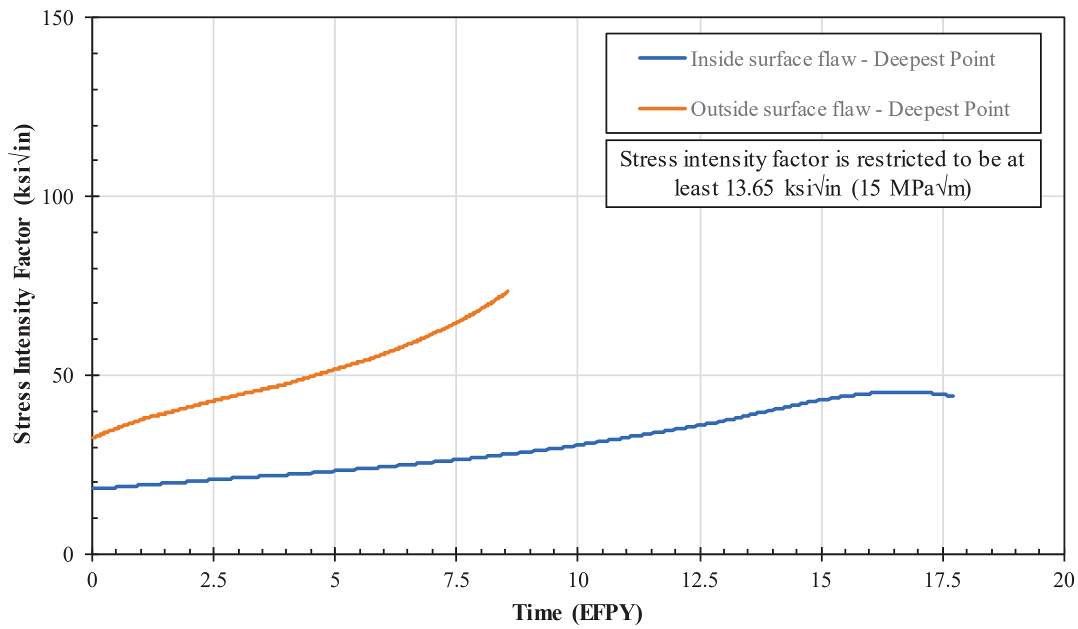

Figure 5. Stress Intensity Factors Calculated for Flaw Deepest Point vs. Time

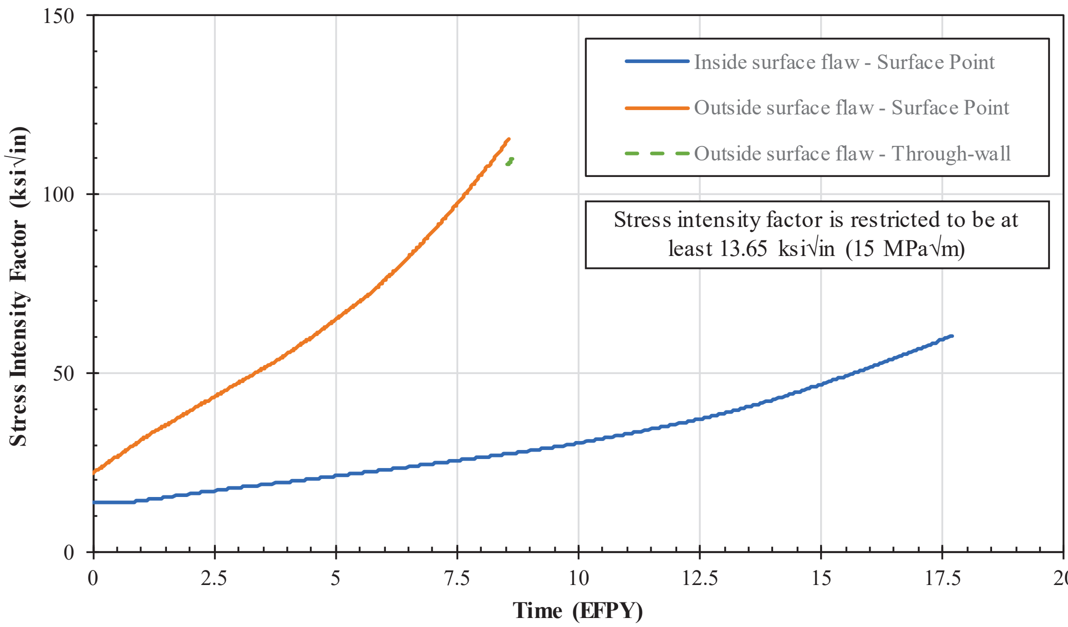

Figure 6. Stress Intensity Factors Calculated for Flaw Surface Point vs. Time

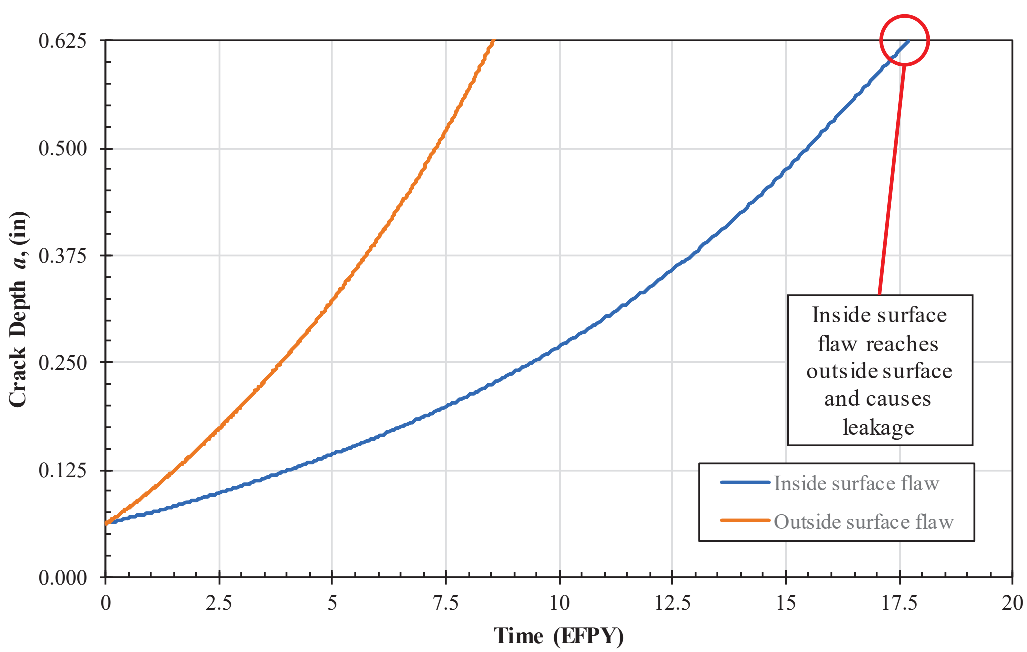

Figure 7. Crack Depth Growth

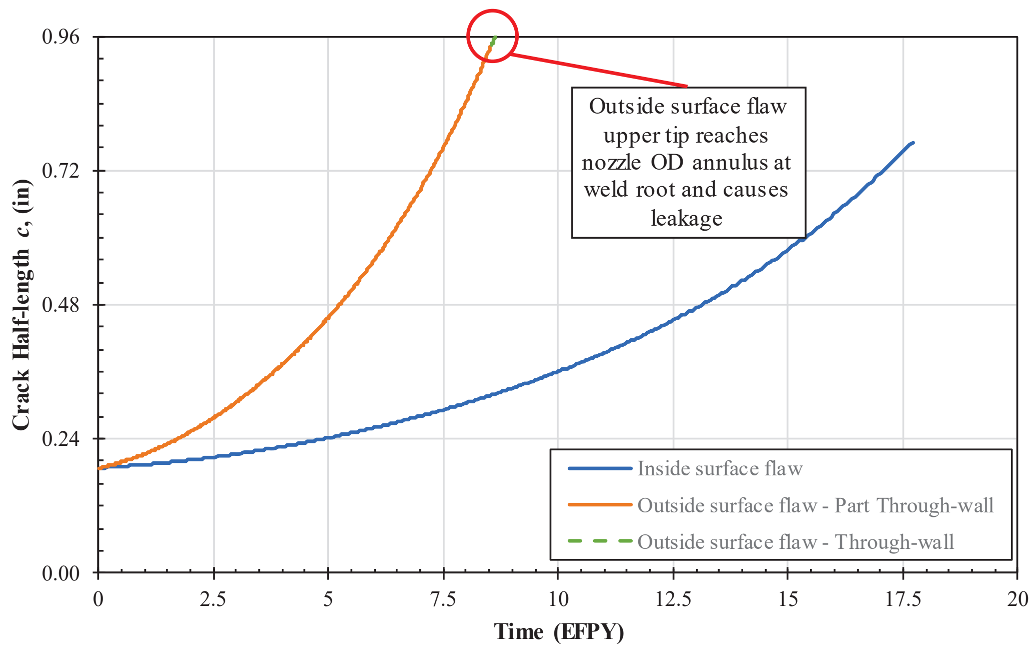

Figure 8. Crack Length Growth

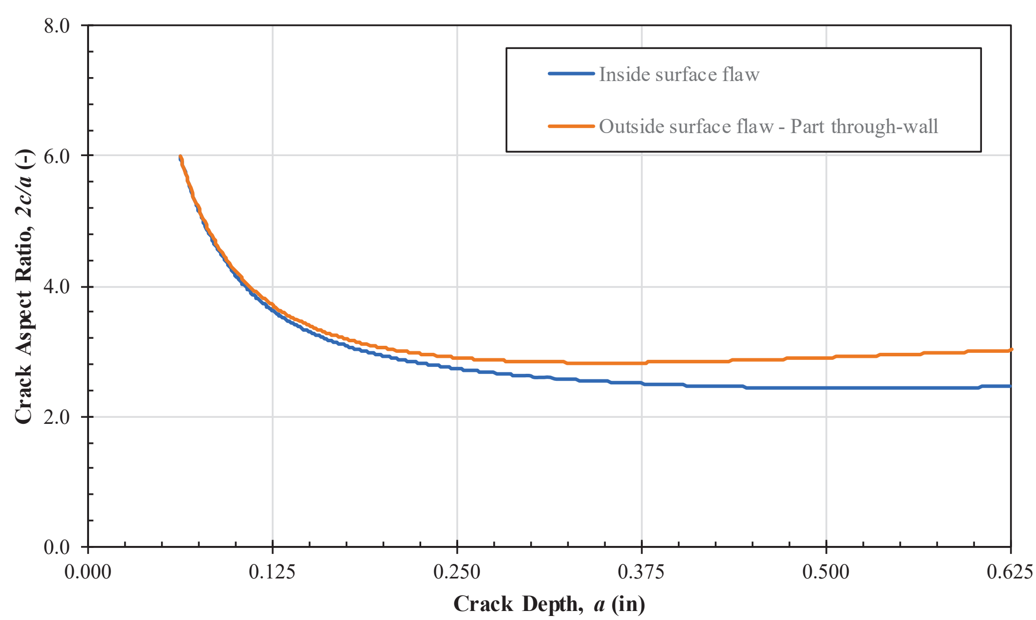

Figure 9. Crack Aspect Ratio Evolution as Function of Crack Depth

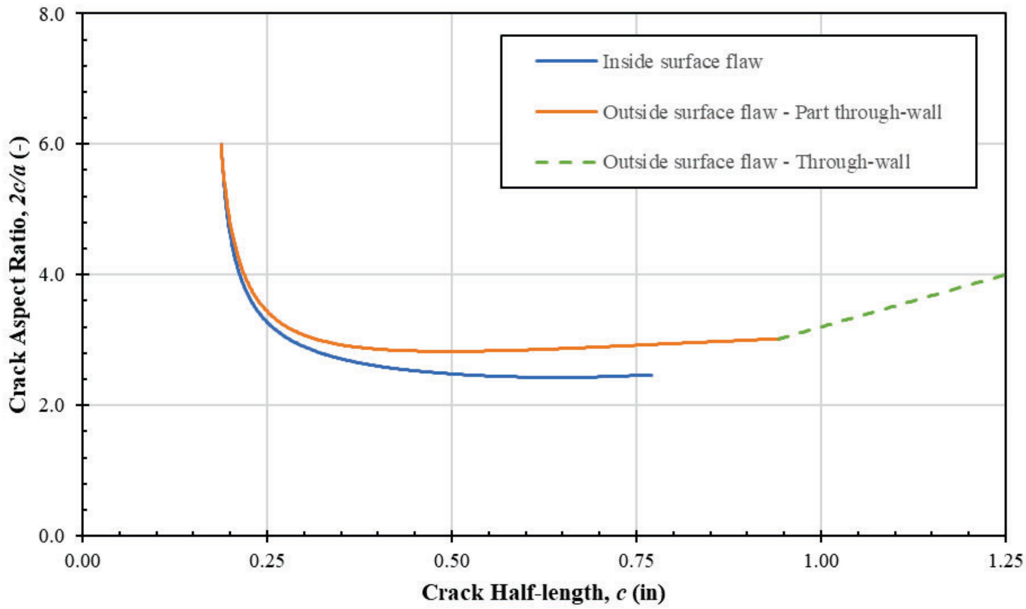

Figure 10. Crack Aspect Ratio Evolution as Function of Crack Length

A CONTENTS OF D-030-2303-00-01 [16]

Directory	Filename	Description
\	C-030-2303-00-01 R0 Crack Growth Calc.xlsx	One Time Use Spreadsheet
Check Files\Coefficient Tables	AxialGsCEA_OD.txt	Influence coefficients for OD axial flaws
	AxialGsCEA.txt	Influence coefficients for ID axial flaws
Check Files\Input Files	030-2303 Cat2 CRDM.csv	Tabular listing of inputs for each case
Check Files\src	calc_K_infl.py	Python code for calculation of stress intensity factors
	crdm_growth_extrap.py	Python code for simulating crack growth
	utilities.py	Python code containing utility functions
Check Files\030-2303 Cat2 CRDM 2023-09-05 (2347)	0 ID - OUT.png 0 OD - OUT.png 16.2 ID-DH - OUT.png 16.2 ID-UH - OUT.png 16.2 OD-DH - OUT.png 16.2 OD-UH (800s) - OUT.png 16.2 OD-UH (900s) - OUT.png 26.2 ID-DH - OUT.png 26.2 ID-UH - OUT.png 26.2 OD-DH - OUT.png 26.2 OD-UH (800s) - OUT.png 26.2 OD-UH (900s) - OUT.png 36.3 ID-DH - OUT.png 36.3 ID-UH - OUT.png 36.3 OD-DH - OUT.png 36.3 OD-UH - OUT.png 48.7 ID-DH - OUT.png 48.7 ID-UH - OUT.png 48.7 OD-DH - OUT.png 48.7 OD-UH - OUT.png	Plots of crack size, crack shape, and stress intensity factors for a single case
	0 ID - OUT.txt 0 OD - OUT.txt 16.2 ID-DH - OUT.txt 16.2 ID-UH - OUT.txt	Text-based printout of crack growth results for a single case

Directory	Filename	Description
	16.2 OD-DH - OUT.txt 16.2 OD-UH (800s) - OUT.txt 16.2 OD-UH (900s) - OUT.txt 26.2 ID-DH - OUT.txt 26.2 ID-UH - OUT.txt 26.2 OD-DH - OUT.txt 26.2 OD-UH (800s) - OUT.txt 26.2 OD-UH (900s) - OUT.txt 36.3 ID-DH - OUT.txt 36.3 ID-UH - OUT.txt 36.3 OD-DH - OUT.txt 36.3 OD-UH - OUT.txt 48.7 ID-DH - OUT.txt 48.7 ID-UH - OUT.txt 48.7 OD-DH - OUT.txt 48.7 OD-UH - OUT.txt	
	Results_Summary.txt	Summary of key results for every case run